

Population Genetics Based Phylogenetics Under Stabilizing Selection for an Optimal Amino Acid Sequence: A Nested Modeling Approach

Jeremy M. Beaulieu^{1,2,3}, Brian C. O'Meara^{2,3}, Russell Zaretzki⁴, Cedric Landerer^{2,3}, Juanjuan Chai^{3,5}, and Michael A. Gilchrist^{2,3,*}

¹Department of Biological Sciences, University of Arkansas, Fayetteville, AR 72701

²Department of Ecology & Evolutionary Biology, University of Tennessee, Knoxville, TN 37996-1610

³National Institute for Mathematical and Biological Synthesis, Knoxville, TN 37996-3410

⁴Department of Business Analytics & Statistics, Knoxville, TN 37996-0532

⁵Current address: 50 Main St, Suite 1039, White Plains, NY 10606

*Corresponding author: *E-mail: mikeg@utk.edu.

Associate Editor: TBD

Abstract

We present a new phylogenetic approach SelAC (Selection on Amino acids and Codons), whose substitution rates are based on a nested model linking protein expression to population genetics. Unlike simpler codon models which assume a single substitution matrix for all sites, our model more realistically represents the evolution of protein coding DNA under the assumption of consistent, stabilizing selection using cost-benefit approach. This cost-benefit approach allows us generate a set of 20 optimal amino acid specific matrix families using just a handful of parameters and naturally links the strength of stabilizing selection to protein synthesis levels, which we can estimate. Using a yeast dataset of 100 orthologs for 6 taxa, we find SelAC fits the data much better than popular models by $10^4 - 10^5$ AICc units. Our results also indicated that nested, mechanistic models better predict observed data patterns highlighting the improvement in biological realism in amino acid sequence evolution that our model provides. Additional parameters estimated by SelAC indicate that a large amount of non-phylogenetic, but biologically meaningful, information can be inferred from existing data. For example, SelAC prediction of gene specific protein synthesis rates correlates well with both empirical ($r=0.33-0.48$) and other theoretical predictions ($r=0.45-0.64$) for multiple yeast species. SelAC also provides estimates of the optimal amino acid at each site. Finally, because SelAC is a nested approach based on clearly stated biological assumptions, future modifications, such as including shifts in the optimal amino acid sequence within or across lineages, are possible.

Key words: Wright-Fisher, stabilizing selection, allele substitution, protein function, gene expression

Article

Introduction

Phylogenetic analyses plays a critical role in most aspects of biology, particularly in the fields of ecology, evolution, paleontology, medicine, and conservation. While the scale and impact of phylogenetic studies have increased substantially over the past two decades, the realism of the mathematical models on which these analyses are based has changed relatively little by comparison. The most popular models of DNA substitution used in molecular phylogenetics are simple nucleotide models that date back to the early 1980's and 90's, e.g. F81, F84, HYK85, TN93, and GTR (see ? for an overview), and are indifferent to the type of sequences they are fitted to. For example, when evaluating protein-coding sequences these models are inherently agnostic with regards to the different amino acid substitutions and their impact on gene function and, as a result, cannot describe the behavior of natural selection at the amino acid or protein level.

Two important and independent attempts to address this critical shortcoming were introduced by ?, commonly abbreviated as GY and ?. These models were explicitly built for protein coding data, assuming that differences in the physicochemical properties between amino acids, or physicochemical distances for short, could affect substitution rates. A number of researchers have used physicochemical based models to make inferences about selection for such properties ?????; however, in terms of tree and/or branch length reconstruction, physicochemical based codon models as originally introduced have rarely been used for empirical data. Instead, the often cited models of ? and ? have served as the basis for an array of simpler and, in turn, more popular ω models that, starting with ??, typically assume an equal fixation probability for *all* non-synonymous mutations. Although often attributed to GY, these later and simpler models were the first to employ the single term ω to model the differences in fixation probability between nonsynonomous and synonomyous changes at all sites. Since their introduction, more complex models have been developed that allow ω to vary between sites or branches (as cited in ?) and include selection on different synonyms for the same amino acid (e.g. ?).

In ?, ?, ? and later studies based on their work, ω is suggested to indicate whether a given site within a protein sequence is under consistent 'stabilizing' ($\omega < 1$) or 'diversifying' ($\omega > 1$) selection. Contrary to popular belief, ω does not describe whether a site is evolving under a constant regime of stabilizing or diversifying selection, but instead how a very particular *selective environment* changes over time. Below we explain how the actual behavior of these models is inconsistent with how 'stabilizing' and 'diversifying' selection are otherwise defined and understood (e.g. see ?).

For example, when $\omega < 1$, synonymous substitutions have a higher substitution rate than any possible non-synonymous substitutions. As a result, the model behaves as if the resident amino acid i at a given site is favored by natural selection. Even when ω is allowed to vary between sites, symmetrical aspects of the model means that for any given site the strength of selection for the resident amino acid i over its 19 alternatives is equally strong regardless of their physicochemical properties. Paradoxically, natural selection for amino acid i persists *until* a substitution for another amino acid, j , occurs. As soon as amino acid j fixes, but not before, selection now favors amino acid j equally over all other amino acids, including amino acid i . This is now the opposite scenario from when i was the resident. Thus, one reasonable interpretation of ω is that it represents the rate at which the selective environment itself changes, and this change in selection at a site perfectly coincides with the fixation of a new amino acid. It is worth distinguishing this from the evolution of proteins to adapt to a shift at one site by compensatory changes at others (??), where a shift from a new amino acid back to the previous one becomes less likely with time. This is in contrast to the ω models where this occurs instantaneously.

Similarly, when $\omega > 1$, synonymous substitutions have a lower substitution rate than any possible non-synonymous substitutions from the resident amino acid. Again due to the model's symmetrical nature, the selection *against* the resident amino acid i is equally strong relative to alternative amino acids. The selection against the resident amino acid i persists until a substitution occurs at which point selection now *favors* amino acid i , as well as the 19 other amino acids, to the same degree i was previously disfavored. Of course, in practice it is unlikely for the non-synonymous rate to be greater than the synonymous substitution rate in the absence of a particular process (e.g., antagonistic coevolution). Given these behaviors, ω based models are likely to only reasonably approximate a narrow set scenarios such as perfectly symmetrical over-/under-dominance or positive/negative frequency dependent selection (???). Further, ω based models implicitly assumes the substitution is on the same timescale as the shifts in the optimal (or pessimal) amino acid. It is for these reasons that ω is best interpreted in a gene-wide context, as opposed to site-specific, because it averages over substitutions across many different sites.

New Approaches

To address these fundamental shortcomings in ω based phylogenetic approaches, we present an approach where selection explicitly favors minimizing the cost-benefit function η of a protein whose relative performance is determined by the order and physicochemical properties of its amino acids. Our approach, which we call Selection on Amino acids and Codons or SelAC, is developed in the same vein as previous phylogenetic applications of the Wright-Fisher process (e.g. ??????????). Similar to ? and ?,

we assume there is a finite set of rate matrices describing the substitution process and that each position within a protein is assigned to a particular rate matrix category. Unlike that work, we assume *a priori* there are 20 different families of rate matrices, one family for when a given amino acid is favored at a site. The key parameters underlying these matrices are shared across genes except for gene expression. As a result, SelAC identifies the amino acid at a particular position within a protein that is favored by natural selection using a simple cost-benefit approach.

While natural selection on protein coding regions can take many forms, one general approach to describing its effects is by relating a codon sequence to the cost of producing the encoded protein and the functional benefit (or potential harm) from translating its sequence. The gene specific cost of protein synthesis can be affected by the amino acids used, the direct and indirect costs of peptide assembly by the ribosome, and the use of chaperones to aid in folding. Importantly, these costs can be computed to varying degrees of realism (e.g. ??). We have previously presented models of protein synthesis costs that, alternatively, take into account the cost of ribosome pausing (?) or premature termination errors (???).

Protein function or ‘benefit’ can be affected by the amino acids at each site and their interactions. Linking amino acid sequence to protein function is a daunting task; thus for simplicity, we assume that for any given desired biological function to be carried out by a protein, that (a) the biological importance of this protein function is invariant across the tree, (b) single optimal amino acid sequence that carries out this function best, and (c) the functionality of alternative amino acid sequences declines with their physicochemical distance from the optimum on a site by site basis.

Beyond fitting the phylogenetic data better than currently available nucleotide and codon models according to model adequacy and AICc, SelAC also makes inferences about other important biological processes. By comparing these inferences to other empirical data, such as we do with protein synthesis data, we can evaluate SelAC’s performance independent of the data it is fitted to. Indeed, SelAC’s assumptions lead to mechanistic and, thus, testable hypothesis about the nature of and relationships between mutation, protein function, gene expression, and rates of evolution. More importantly, alternative hypotheses could be used in place of ours and, in turn, phylogenetic and other types of data could be used to evaluate the support of these alternative models. Our hope is that by moving away from the more phenomenological models we can better connect population genetics, molecular biology, and phylogenetics allowing each area inform the others more effectively.

Results

The SelAC model requires the construction of gene and amino acid specific substitution matrices that uses a submodel nested within our substitution model. This requires only a handful of genome-wide parameters such as nucleotide specific mutation rates $\mu_{i,j}$, which are scaled by effective population size N_e , amino acid side chain physicochemical weighting parameters α_c , α_p , and α_v , and a gamma distribution shape parameter α_G describing the distribution of site sensitivities G . In addition to these genome-wide parameters, the model requires a gene-specific functionality expression parameter that describes the average rate at which the protein's functionality is produced by the organism or a gene's 'average functionality production rate' ψ . By linking transition rates $q_{i,j}$ to gene expression in the form of protein synthesis rate ϕ , our approach allows use of the same model for genes under varying degrees of stabilizing selection. Specifically, we assume the strength of stabilizing selection for an optimal sequence, \vec{a}^* , is proportional to ψ , which we can estimate for each gene.

We first evaluated the performance of our codon model by simulating datasets and estimating the bias of the inferred model parameters from these data. Overall, the simulation results indicated that our SelAC model can reasonably recover the known values of the generating model (Figure ???). This includes not only the parameters in SelAC, but also the optimal amino acids for a given sequence as well as the estimates of the branch lengths. There are, however, a few observations to note. First, the ability to accurately recover the true optimal amino acid sequence \vec{a}^* will largely depend on the magnitude of the realized average protein synthesis rate of the gene ϕ , which is the target functionality rate ψ divided by the functionality of the observed amino acid sequence $\mathbf{B}(\vec{a})$. This is, of course, intuitive, given that ψ sets the strength of stabilizing selection towards an optimal amino acid at a site. However, the inclusion of between site variation in selection via the shape parameter α_G into SelAC generally increase our estimates of ψ as well as improve our ability to recover the optimal amino acids \vec{a}^* . This is true even for the gene with the lowest baseline ψ . Second, we found a strong downward bias in estimates of α_G , which actually translates to greater variation among the rate categories. The choice of a gamma distribution to represent site-specific variation in sensitivity was based on mathematical convenience and convention, rather than on biological reality. Further, given the fact that the density of the gamma distribution is infinite at $G=0$ when $\alpha_G < 1$, imputing site specific G values will be an issue in these scenarios. Nevertheless, we suspect that this downward estimation bias of α_G is in large part due to the difficulty in determining the baseline ψ for a given gene and the value of α_G that globally satisfies the site-specific variation in sensitivity across all genes, as indicated by the slight upward bias in estimates of ψ (see Figure ??).

153 In regards to model fit in an empirical setting, our results clearly indicated that linking the
 154 strength of stabilizing selection for the optimal sequence to gene expression substantially improves
 155 our model fit. Further, including the shape parameter α_G for the random effects term $G \sim$
 156 $\text{Gamma}(\text{shape}=\alpha_G, \text{rate}=\alpha_G)$ to allow for heterogeneity in this selection between sites within a gene
 157 improves the ΔAICc of SelAC+ Γ over the simpler SelAC models by over 22,000 AIC units. Using either
 158 ΔAICc or AIC_w as our measure of model support, the SelAC models fit extraordinarily better than
 159 GTR + Γ , GY, or FMutSel (Table ??). This is in spite of the need for estimating the optimal amino
 160 acid at each position in each protein, which accounts for 49,881 additional model parameters. Even when
 161 compared to the next most parameter rich codon model in our model set, FMutSel (with 178 parameters),
 162 SelAC+ Γ model shows over 160,000 AIC unit improvement over FMutSel. SelAC models also appeared
 163 to outperform, based on likelihood, and reported AIC and AICc from each program, the codon models
 164 in IQtree (?). See Table ?? for results.

165 We note our use of AICc, as opposed to the standard AIC, in the above model comparisons. At the
 166 outset of our study it was unclear what the appropriate sample size, n , when comparing models of
 167 sequence evolution. Building upon the work of ?, our simulations suggest that using the number of taxa
 168 times the number of sites as the sample size correction performed best as a small sample size correction
 169 for estimating Kullback-Liebler distance in phylogenetic models (Supporting Materials). This also has an
 170 intuitive appeal. In models that have at least some parameters shared across sites and some parameters
 171 shared across taxa, increasing the number of sites and/or taxa should be adding more samples for
 172 the parameters to estimate. This is consistent considering how likelihood is calculated for phylogenetic
 173 models: the likelihood for a given site is the sum of the probabilities of each observed state at each
 174 tip, which is then multiplied across sites. It is arguable that the conventional approach in comparative
 175 methods is calculating AICc in the same way. That is, if only one column of data (or “site”) is examined,
 176 as remains remarkably common in comparative methods, when we refer to sample size, it is technically
 177 the number of taxa multiplied by number of sites, even though it is referred to simply as the number of
 178 taxa.

179 With respect to estimates of ϕ within SelAC, they were strongly correlated with both empirical
 180 measurements (Pearson $r=0.33-0.48$) and theoretical predictions (Pearson $r=0.45-0.64$) of gene
 181 expression (Figure ?? and Figures S1-S2, respectively). These correlations are remarkable given that
 182 they were uncovered using only codon sequences. The estimate of the α_G parameter, which controls
 183 the shape of the site-specific, gamma-distributed, variation in sensitivity of the protein’s functionality,
 184 indicated a moderate level of variation in gene expression among sites. Our estimate of $\alpha_G = 1.36$,

185 produced a distribution of sensitivity terms G ranged from 0.342-7.32, but with more than 90% of the
 186 weight for a given site-likelihood being contributed by the 0.342 and 1.50 rate categories. In simulation,
 187 however, of all the parameters in the model, only α_G showed a consistent bias, in that the MLE were
 188 generally lower than their actual values (see Supporting Materials). Other parameters in the model, such
 189 as the Grantham weights, provide an indication as to the physicochemical distance between amino acids.
 190 Our estimates of these weights only strongly deviate from Grantham's ? original estimates in regards
 191 to composition weight, α_c , which is the ratio of non-carbon atoms in the end groups or rings to the
 192 number of carbon atoms in side chains. Our estimate of the composition weighting factor of $\alpha_c=0.459$ is
 193 1/4th the value estimate by Grantham which suggests that the substitution process is less sensitive to
 194 this physicochemical property when shared ancestry and variation in stabilizing selection are taken into
 195 account.

196 It is important to note that the nonsynonymous/synonymous mutation ratio, or ω , which we estimated
 197 for each gene under the FMutSel model strongly correlated with our estimates of $\phi' = \psi' / \mathbf{B}$ where \mathbf{B}
 198 depends on the sequence of each taxa. In fact, ω showed similar, though slightly reduced correlations,
 199 with the same empirical estimates of gene expression described above (Figure ??) This would give the
 200 impression that the same conclusions could have been gleaned using a much simpler model, both in terms
 201 of the number of parameters and the assumptions made. However, as we discussed earlier, not only is
 202 this model greatly restricted in terms of its biological feasibility, SelAC clearly performs better in terms
 203 of its fit to the data and biological realism.

204 For example, when we simulated the sequence for *S. cerevisiae*, starting from the ancestral sequence
 205 under both GTR + Γ and FMutSel, the functionality of the simulated sequence, defined as protein
 206 function in relation to the physicochemical distance from each amino acid to the optimal, moves away
 207 from the observed sequence. By contrast, SelAC remains near the functionality of the observed sequence
 208 (Figure ??b). This is somewhat unsurprising, given that both GTR + Γ and FMutSel are agnostic
 209 to the functionality of the gene, but it does highlight the improvement in biological realism in amino
 210 acid sequence evolution that SelAC provides. We do note that the adequacy of the SelAC model does
 211 vary among individual taxa, and does not always match the observed functionality. For instance, our
 212 simulations of *S. castellii* gene function is consistently higher than estimated from the data (Figure ??c).
 213 We suspect this is an indication that assuming a single set of optimal amino acid across all taxa is too
 214 simplistic. However, we cannot rule out violations of SelAC's other model assumptions such as, a single
 215 set of Grantham weights, a single α_G , or reductions in protein functionality \mathbf{B} being solely a function of
 216 physicochemical distances d between sites.

Discussion

A central goal in evolutionary biology is to quantify the nature, strength, and, ultimately, shifts in the forces of natural selection relative to genetic drift and mutation. As data set size and complexity increase, so does the amount of potential information on these forces and their dynamics. As a result, there is a need for more complex and realistic models to accomplish this goal (?????). Although extremely popular due to their elegance and computational efficiency, the utility of ω based models in helping us reach this goal is substantially more limited than commonly recognized. Because these ω models use a single substitution matrix, they are only applicable for situations in which the substitution process and shifts in the selective environment are intrinsic to the sequence, such as with positive or negative frequency dependent selection; these models do not describe stabilizing or diversifying selection as commonly envisioned (??).

Starting with ?, a number of researchers have developed methods for linking heterogenous or site-specific selection on protein sequence and phylogenetics (e.g. ?????????). ? calculated a vector of 20 expected amino acid frequencies for each amino acid site, making it the most general and most parameter rich of these methods. This generality, however, comes at the cost of being purely descriptive; there is no explicit biological mechanism proposed to explain the site specific amino acid frequencies estimated. By grouping together amino sites with similar evolutionary behaviors, ? and ? retained the descriptive nature of ? work while greatly reduced the number of model parameters needed.

SelAC follows in this tradition of using multiple substitution matrices, but includes some key advances. First, by nesting a model of a sequence's cost-benefit function \mathbf{C}/\mathbf{B} within a broader model, SelAC allows us to formulate and test a hierarchical, mechanistic models of stabilizing selection. More precisely, our nested approach allows us to relax the assumption that physicochemical deviations from the optimal sequence \vec{a}^* are equally disruptive at all sites within a protein. Indeed, SelAC results are consistent with the idea that the strength of stabilizing selection against physicochemical deviations from \vec{a}^* varies between sites ($\Delta\text{AICc} = 20,983$; Table ??). Second, because our substitution matrices are built on a formal description of a sequence's cost-benefit function \mathbf{C}/\mathbf{B} , we are able to efficiently parameterize 20 different matrices using a relatively small number of genome-wide parameters – e.g. our physicochemical weightings, α_c , α_p , and α_v , and the shape parameter α_G for the distribution of selective strength G and one gene specific expression parameter ψ . While the \mathbf{C}/\mathbf{B} function on which SelAC currently rests is very simple, nevertheless, it leads to a dramatic increase in our ability to explain the sequence data we analyzed. Importantly, because SelAC uses a formal description of a sequence's \mathbf{C}/\mathbf{B} , replacing our assumptions with more sophisticated ones in the future is relatively straightforward. Third, our use of

248 nested models also allows us to make biologically meaningful and testable predictions. By linking a
249 gene's expression level to the strength of purifying selection it experiences, we are able to provide coarse
250 estimates of gene expression. This also suggests that the anticorrelation between ω and gene expression
251 is a proxy for the nature of selection on a sequence.

252 Thus, we believe our cost-benefit approach to be a substantial advance of the more simplistic ω models,
253 is complementary to the work of others in the field (e.g. ??), and, in turn, lays the foundation for more
254 realistic work in the future. For instance, by assuming there is an optimal amino acid for each site, SelAC
255 naturally leads to a non-symmetrical and, thus, more cogent model of protein sequence evolution. Because
256 the strength of selection depends on an additive function of amino acid physicochemical properties, an
257 amino acid more similar to the optimum has a higher probability of replacing a more dissimilar amino
258 acid than the converse situation. Further, SelAC does not assume the system is always at the optimum
259 or pessimum point of the fitness landscape, as occurs when $\omega < 1$ or > 1 , respectively.

260 Importantly, the cost-benefit approach underlying SelAC allows us to link the strength of selection on
261 a protein sequence to its gene's expression level. Despite its well recognized importance in determining
262 the rate of protein evolution (e.g. ??), phylogenetic models have ignored the fact that expression levels
263 vary between genes. In order to link gene expression and the strength of stabilizing selection on protein
264 sequences, we simply assume that the strength of selection on a gene is proportional to the average
265 protein synthesis rate of the gene.

266 One possible mechanism with some theoretical and empirical support which generates a linear
267 relationship between the strength of selection and gene expression is the assumption of compensatory gene
268 expression (???????). That is, the assumption that any reduction in protein function is compensated
269 for by an increase in the protein's production rate and, in turn, abundance. For example, a mutation
270 which reduces the functionality of the protein to 90% of the optimal protein, would require $1/0.9 = 1.11$
271 of these suboptimal proteins to be produced relative to the optimal protein in order to maintain the
272 same amount of that protein's functionality in the cell. Because the energetic cost of an 11% increase
273 in a protein's synthesis rate is proportional to its target synthesis rate, our assumptions naturally link
274 changes in protein functionality and changes in gene expression and its associated costs. Such a response
275 has been shown when error rates during protein production increases, however, the generality of such a
276 response has to be determined (?). Further, our model does not consider additional costs such as those
277 imposed by misfolded proteins ?. Nevertheless, the fact that our method allows us to explain 13-23% of the
278 variation in gene expression measured using RNA-Seq, suggests that our assumption of cell compensation
279 via increased expression is a reasonable starting point.

Furthermore, by linking expression and selection, SelAC provides a natural framework for combining information from protein coding genes with very different rates of evolution; from low expression genes providing information on shallow branches to high expression genes providing information on deep branches. This is in contrast to a more traditional approach of concatenating gene sequences together, which is equivalent to assuming the same average functionality production rate ψ for all of the genes, or more recent approaches where different models are fitted to different genes. Our results indicate that including a gene specific ψ value vastly improves SelAC fits (Table ??). Perhaps more convincingly, we find that the target functionality production rate ψ and the realized average protein synthesis rate $\phi = \psi/\mathbf{B}$ are reasonably well correlated with laboratory measurements and theoretical predictions of gene expression (Pearson $r=0.34-0.64$; Figures ??, ??, and ??). The idea that quantitative information on gene expression is embedded within intra-genomic patterns of synonymous codon usage is well accepted; our work shows that this information can also be extracted from comparative data at the amino acid level.

Of course, given the general nature of SelAC and the complexity of biological systems, other biological forces besides selection for reducing energy flux likely contribute to intergenic variation in the magnitude of stabilizing selection. Similarly, other physicochemical properties besides composition, volume, and charge likely contribute to site specific patterns of amino acid substitution. For example, ? have developed substitution matrices using various physicochemical properties. Thus, a larger and more informative set of physicochemical weights might improve our model fit and reduce the noise in our estimates of realized protein synthesis rates ϕ . Even if other physicochemical properties are considered, the idea of a consistent, genome wide physicochemical weighting of these terms seems highly unlikely. Since the importance of an amino acid's physicochemical properties likely changes with its position in a folded protein, one way to incorporate such effects is to test whether the data supports multiple sets of physicochemical weights for either subsets of genes or regions within genes, rather than a single set.

Both of these points highlight the advantage of the detailed, mechanistic modeling approach underlying SelAC. Because there is a clear link between protein expression, synthesis cost, and functionality, SelAC can be extended by increasing the realism of the mapping between these terms and the coding sequences being analyzed. For example, SelAC currently assumes the optimal amino acid for any site is fixed along all branches. This assumption can be relaxed by allowing the optimal amino acid to change during the course of evolution along a branch. From a computational standpoint, the additive nature of selection between sites is desirable because it allows us to analyze sites within a gene largely independently of each other. From a biological standpoint, this additivity between sites ignores any non-linear interactions

312 between sites, such as epistasis, or between alleles, such as dominance. Thus, our work can be considered
313 a first step to modeling these more complex scenarios.

314 For example, our current implementation ignores any selection on synonymous codon usage bias (CUB)
315 (c.f. ??). Including such selection is tricky because introducing the site-specific cost effects of CUB, which
316 is consistent with the hypothesis that codon usage affects the efficiency of protein assembly or **C**, into a
317 model where amino acids affect protein function or **B**, results in a cost-benefit ratio **C/B** with epistatic
318 interactions between all sites. These epistatic effects can likely be ignored under certain conditions or
319 reasonably approximated based on an expectation of codon specific costs (e.g. ?). Nevertheless, it is
320 difficult to see how one could identify such conditions without modeling the way in which codon and
321 amino acid usage affects **C/B**.

322 This work also points out the potential importance of further investigation into model choice in
323 phylogenetics. For likelihood models, use of AICc has become standard. However, how one determines the
324 appropriate number of data points in a model is more complicated than generally recognized. Common
325 sense suggests that dataset size is increased by adding taxa and/or sites. In other words, a dataset of 1000
326 taxa and 100 sites must have more information on substitution models than a dataset of 4 taxa and 100
327 sites. Our simple analyses agree that the number of observations in a dataset (number of sites \times number
328 of taxa) should be taken as the sample size for AICc, but this conclusion likely only applies when there
329 is sufficient independence between taxa. For instance, one could imagine a phylogeny where one taxon is
330 sister to a polytomy of 99 taxa that have zero length terminal branches. Absent measurement error or
331 other intraspecific variation, one would have 100 species but only two unique trait values, and the only
332 information about the process of evolution comes from what happens on the path connecting the lone
333 taxon to the polytomy. Although this is a rather extreme example, it seems prudent for researchers to
334 use a simulation based approach similar to the one we take here to determine the appropriate means for
335 calculating the effective number of data points in their data.

336 There are still significant shortcomings in the approach outlined here. Most worrisome are biological
337 oversimplifications in SelAC. For example, at its heart, SelAC assumes that suboptimal proteins can
338 be compensated for, at a cost, simply by producing more of them. However, this is likely only true
339 for proteins reasonably close to the optimal sequence. Different enough proteins will fail to function
340 entirely: the active site will not sufficiently match its substrates, a protein will not properly pass through
341 a membrane, and so forth. Yet, in our model, even random sequences still permit survival, just requiring
342 more protein production. Another deficiency is the assumption of site independence and unchanging
343 optimal amino acids through time, neither of which matches reality (??). We assume single nucleotide

changes only, despite evidence from ?? that better fit can be accomplished by allowing instantaneous mutations of multiple nucleotides simultaneously. Like the other oversimplifications previously discussed, these assumptions can be relaxed through further extension of this model.

A deeper potential issue comes from the nature of model fitting itself. Because SelAC is built on very particular assumptions - the exact combination of physicochemical properties favored by selection matches that of an amino acid, sites evolve independently of one another, the cell's response to suboptimality is to produce more proteins, etc - it is likely these assumptions are violated in many, if not most, cases. While all models are incomplete descriptions of reality and, thus, wrong (?), our aim with SelAC is to provide a model that is 'less wrong' (?). Because SelAC's assumptions result in a model that is more consistent with the data, our analyses supports this idea. While 'less wrong', caution should be taken when interpreting SelAC's model parameters since the model itself is admittedly incomplete. In addition, other biological mechanisms could result in similar, if not identical, mathematical representations (Goldberg and Rabosky, 2013) which, in turn, illustrates one limit to comparative sequence analysis.

There are also deficiencies in our implementation. Though reasonable to use for a given topology with 10's of species, it is currently too slow for practical use for tree search. Our work serves as a proof of concept, or of utility for targeted questions where a more realistic model may be of use (placement of particular taxa, for example). Future work will encode SelAC models into a variety of mature, popular tree-search programs. SelAC also represents a challenging optimization problem: the nested models reduce parameter complexity vastly, but there are still numerous parameters to optimize, including the discrete parameter of the optimal amino acid at each site. One way to avoid the use of discrete parameters at the expense of more of them would be to have SelAC estimate the optimum physicochemical values on a per site basis rather than a specific amino acid. While this would increase the number of parameters estimated, it would have the practical advantage of continuous parameter optimization rather than discrete. More importantly, biologically such a model would be more realistic (as it is the properties that selection "sees", not the identity of the amino acid itself).

In spite of these difficulties, SelAC represents an important step in uniting phylogenetic and population genetic models (?). Most work in this area use a given tree to make inferences about the nature or distribution of selection coefficients ?????, e.g.. While the work of ?????? does involve tree inferences, are all models of constant, stabilizing selection, SelAC can be generalized further to include diversifying selection. Specifically, by letting SelAC's sensitivity term G , which we now assume is ≥ 0 , to take on negative values, SelAC will behave as if there is a pessimal, rather than optimal, amino acid for the given

375 site. In this diversifying selection scenario, amino acids with physicochemical qualities more dissimilar to
376 the pessimal amino acid are increasingly favored, potentially resulting in multiple fitness peaks.

377 The ability to extend our model and, in turn, sharpen our thinking about the nature of natural selection
378 on amino acid sequences illustrates the value of moving from descriptive to more mechanistic models in
379 general and phylogenetics in particular. How frequently diversifying selection of this nature occurs is
380 an open, but addressable, question. Regardless of the frequency at which diversifying selection occurs,
381 another question of interest to evolutionary biologists is, “How often does the optimal/pessimal amino
382 sequence change along any given branch?” Due to its mechanistic nature, SelAC can also be extended
383 to include changes in the optimal/pessimal sequence over a phylogeny using a hidden Markov modelling
384 approach (???, for an explicit shift the optimal sequence see ?). Extending SelAC in these ways, will
385 allow researchers to explicitly model shifts in selection on protein sequences and, in turn, quantify their
386 frequency and magnitude thus deepening our understanding of biological evolution. Such approaches
387 would be challenging using non-mechanistic and parameter rich models which infer up to 19 different
388 parameters per site category ?????.

389 In summary, SelAC allows biologically relevant population genetic parameters to be estimated from
390 phylogenetic information, while also dramatically improving fit and accuracy of phylogenetic models. By
391 explicitly modeling the optimal/pessimal sequence of a gene, SelAC can be extended to include shifts
392 in the optimal/pessimal sequence over evolutionary time. Moreover, it demonstrates that there remains
393 substantially more information in the coding sequences used for phylogenetic analysis than other methods
394 can access. Given the enormous amount of efforts expended to generate sequence datasets, it makes sense
395 for researchers to continue developing more realistic models of sequence evolution in order to extract the
396 biological information embedded in these datasets. The cost-benefit model we develop here is just one of
397 many possible paths of mechanistic model development.

398 **Materials & Methods**

399 **Overview**

400 We model the substitution process as a classic Wright-Fisher process which includes the forces of
401 mutation, selection, and drift (???????). For simplicity, we ignore linkage effects and, as a result of this
402 and other assumptions, sequences evolve in a site independent manner.

403 Because SelAC requires twenty families of 61×61 matrices, the number of parameters needed to
404 implement SelAC would, without further assumptions, be extremely large (i.e. on the order of 74,420
405 parameters). To reduce the number of parameters needed, while still maintaining a high degree of

biological realism, we construct our gene and amino acid specific substitution matrices using a submodel nested within our substitution model, similar to approaches in ???.

One advantage of a nested modeling framework is that it requires only a handful of genome-wide parameters such as nucleotide specific mutation rates (scaled by effective population size N_e), amino acid side chain physicochemical weighting parameters, and a shape parameter describing the distribution of site sensitivities. In addition to these genome-wide parameters, SelAC requires a gene g specific functionality expression parameter ψ_g which describes the average rate at which the protein's functionality is produced by the organism or a gene's 'average functionality production rate' for short (for notational simplicity, we will ignore the gene specific indicator $_g$, unless explicitly needed). Currently, ψ is fixed across the phylogeny, though relaxing this assumption is a goal of future work. The gene specific parameter ψ is multiplied by additional model terms to make a composite term ψ' which scales the strength and efficacy of selection for the optimal amino acid sequence relative to drift (see Implementation below). In terms of the functionality of the protein encoded, we assume that for any given gene there exists an optimal amino acid sequence \vec{a}^* and that, by definition, a complete, error free peptide consisting of \vec{a}^* provides one unit of the gene's functionality. We also assume that natural selection favors genotypes that are able to synthesize their proteome more efficiently than their competitors and that each savings of an high energy phosphate bond per unit time leads to a constant proportional gain in fitness A_0 . SelAC also requires the specification (as part of parameter optimization) of an optimal amino acid a^* at each position within a coding sequence. This requirement of one a^* per site makes our \vec{a}^* the largest category of parameters SelAC estimates. Despite the need to specify a^* for each site, because we use a submodel to derive our substitution matrices, SelAC estimates a relatively small number of the parameters when compared to more general approaches where the fitness of each amino acid is allowed to vary freely of any physicochemical properties (???).

As with other phylogenetic methods, SelAC generates estimates of branch lengths and nucleotide specific mutation rates. In addition, the method can also be used to make quantitative inferences on the optimal amino acid sequence of a given protein as well as the realized average synthesis rate of each protein used in the analysis. The mechanistic basis of SelAC also means it can be easily extended to include more biological realism and test more explicit hypotheses about sequence evolution.

Mutation Rate Matrix μ

We begin with a 4x4 nucleotide mutation matrix μ that describes mutation rates between different bases and, in turn, different codons. For our purposes, we rely on the general unrestricted model (UNREST from ?) because it imposes no constraints on the instantaneous rate of change between any pair of

438 nucleotides. More constrained models, such as the Jukes-Cantor (JC), Hasegawa-Kishino-Yano (HKY),
 439 or the general time-reversible model (GTR), could also be used.

440 The 12 parameter UNREST model defines the relative rates of change between a pair of nucleotides.
 441 Thus, we arbitrarily set the G→T mutation rate to 1, resulting in 11 free mutation rate parameters in the
 442 4x4 mutation nucleotide mutation matrix. The nucleotide mutation matrix is also scaled by a diagonal
 443 matrix $\boldsymbol{\pi}$ whose entries, $\pi_{i,i}$, correspond to the equilibrium frequencies of each base. These equilibrium
 444 nucleotide frequencies are determined by analytically solving $\boldsymbol{\pi} \times \mathbf{Q} = 0$. We use this \mathbf{Q} to populate a
 445 61×61 codon mutation matrix $\boldsymbol{\mu}$, whose entries $\mu_{i,j}$ $i \neq j$ describes the mutation rate from codon i to j
 446 and $\mu_{i,i} = -\sum_j \mu_{i,j}$. We generate this matrix using a “weak mutation” assumption, such that evolution is
 447 mutation limited, codon substitutions only occur one nucleotide at a time. As a result, the rate of change
 448 between any pair of codons that differ by more than one nucleotide is zero.

449 While the overall model does not assume equilibrium, we still need to scale our mutation matrices μ
 450 by a scaling factor S . As traditionally done, we rescale our time units such that at equilibrium, one unit
 451 of branch length represents one expected mutation per site (which equals the substitution rate under
 452 neutrality). More explicitly, $S = -(\sum_{i \in \text{codons}} \mu_{i,i} \pi_{i,i})$ where the final mutation rate matrix is the original
 453 mutation rate matrix multiplied by $1/S$.

454 **Protein Synthesis Cost-Benefit Function η**

455 SelAC links fitness to the product of the cost-benefit function of a gene η and the organism’s average
 456 target synthesis rate of the functionality provided by gene ψ . As a result, the average flux energy an
 457 organism spends to meet its target functionality provided by the gene is $\eta \times \psi$. Compensatory changes
 458 that allow an organism to maintain functionality even with loss of one or both copies of a gene are
 459 widespread. There is evidence of compensation for protein function. Metabolism with gene expression
 460 models (ME-models) link those factors to successfully make predictions about response to perturbations
 461 in a cell (??). For example, an ME-model for *E. coli* successfully predicted gene expression levels in vivo
 462 (?). Here we assume that for finer scale problems than entire loss (for example, a 10% loss of functionality)
 463 the compensation is more production of the protein. The particular type of dosage compensansation assumed
 464 by SelAC in respondse to stress (e.g. reduced functionality) is commonly assumed in microbial ecology
 465 (??). Our assumption is also consistent with the Michaelis-Menten enzyme kinetics. Moreover, there is
 466 evidence that mutations can influence expression level, though this does not always match our expression
 467 compensation assumption (??). In order to link genotype to our cost-benefit function $\eta = \mathbf{C}/\mathbf{B}$, we begin
 468 by defining our benefit function \mathbf{B} .

469 *Benefit:* Our benefit function \mathbf{B} measures the functionality of the amino acid sequence \vec{a}_i encoded by a
 470 set of codons \vec{c}_i , i.e. $a(\vec{c}_i) = \vec{a}_i$ relative to that of an optimal sequence \vec{a}^* . By definition, $\mathbf{B}(\vec{a}^*|\vec{a}^*) = 1$ and
 471 $\mathbf{B}(\vec{a}_i|\vec{a}^*) < 1$ for all other sequences. We assume all amino acids within the sequence contribute to protein
 472 function and that this contribution declines as an inverse function of physicochemical distance from each
 473 amino acid to the optimal one. Formally, we assume that

$$\mathbf{B}(\vec{a}|\vec{a}^*) = \left(\frac{1}{n} \sum_{p=1}^n (1 + G_p d(a_p, a_p^*)) \right)^{-1} \quad (1)$$

474 where n is the length of the protein, $d(a_p, a_p^*)$ is a weighted physicochemical distance between the amino
 475 acid encoded at a given position p and a_p^* is the optimal amino acid for that position. There are many
 476 possible measures for physiochemical distance; we use ? distances by default, though others may be
 477 chosen. For simplicity, we assume all nonsense mutations are lethal by defining the the physicochemical
 478 distance between a stop codon and a sense codon as ∞ . The term G_p describes the sensitivity of the
 479 protein's function to physicochemical deviation from the optimum at site position p . We assume that
 480 $G_p \sim \text{Gamma}(\text{shape} = \alpha_G, \text{rate} = \alpha_G)$ in order to ensure $\mathbb{E}(G_p) = 1$. Given the definition of the Gamma
 481 distribution, the variance in G_p is equal to $\text{shape}/\text{rate}^2 = 1/\alpha_G$. We note that at the limit of $\alpha_G \rightarrow \infty$, the
 482 model becomes equivalent to assuming uniform site sensitivity where $G_p = 1$ for all positions p . Further,
 483 $\mathbf{B}(\vec{a}_i|\vec{a}^*)$ is inversely proportional to the average physicochemical deviation of an amino acid sequence
 484 \vec{a}_i from the optimal sequence \vec{a}^* weighted by each site's sensitivity to this deviation. $\mathbf{B}(\vec{a}_i|\vec{a}^*)$ can be
 485 generalized to include second and higher order terms of the distance measure d .

486 *Cost:* Protein synthesis involves both direct and indirect assembly costs. Direct costs consist of the high
 487 energy phosphate bonds $\sim P$ of ATPs or GTPs used to assemble the ribosome on the mRNA, charge
 488 tRNA's for elongation, move the ribosome forward along the transcript, and terminate protein synthesis.
 489 As a result, direct protein assembly costs are the same for all proteins of the same length. Indirect costs of
 490 protein assembly are potentially numerous and could include the cost of amino acid synthesis as well the
 491 cost and efficiency with which the protein assembly infrastructure such as ribosomes, aminoacyl-tRNA
 492 synthetases, tRNAs, and mRNAs are used. When these indirect costs are combined with sequence specific
 493 benefits, the probability of a mutant allele fixing is no longer independent of the rest of the sequence (?)
 494 and, as a result, model fitting becomes substantially more complex. Thus for simplicity, in this study we

495 ignore indirect costs of protein assembly that vary between genotypes and define,

$$\begin{aligned} \mathbf{C}(\vec{c}_i) &= \text{Direct energetic cost of protein synthesis.} \\ &= A_1 + A_2 n \end{aligned}$$

496 where, A_1 and A_2 represent the direct cost, in high energy phosphate bonds, of ribosome initiation and
497 peptide elongation, respectively, where $A_1 = A_2 = 4 \sim P$.

498 **Defining Physicochemical Distances**

499 Assuming that functionality declines with an amino acid a_i 's physicochemical distance from the
500 optimum amino acid a^* at each site provides a biologically defensible way of mapping genotype to protein
501 function that requires relatively few free parameters. In addition, SelAC naturally lends itself to model
502 selection since one could compare the quality of SelAC fits using different mixtures of physicochemical
503 properties. Following (?), we focus on using composition c , polarity p , and molecular volume v of each
504 amino acid's side chain residue to define our distance function, but the model and its implementation
505 can flexibly handle a variety of properties. We use the Euclidian distance between residue properties
506 where each property c , p , and v has its own weighting term, α_c , α_p , α_v , respectively, which we refer to as
507 'Grantham weights'. Because physicochemical distance is ultimately weighted by a gene's specific average
508 protein synthesis rate ψ , another parameter we estimate, there is a problem with parameter identifiability.
509 The scale of gene expression is affected by how we measure physicochemical distances which, in turn,
510 is determined by our choice of Grantham weights. As a result, by default we set $\alpha_v = 3.990 \times 10^{-4}$, the
511 value originally estimated by Grantham, and recognize that our estimates of α_c and α_p and ψ are scaled
512 relative to this choice for α_v . More specifically,

$$\begin{aligned} d(a_i, a^*) &= \left(\alpha_c [c(a_i) - c(a^*)]^2 + \alpha_p [p(a_i) - p(a^*)]^2 + \right. \\ &\quad \left. \alpha_v [v(a_i) - v(a^*)]^2 \right)^{1/2}. \end{aligned}$$

513 **Linking Protein Synthesis to Allele Substitution**

514 Next we link the protein synthesis cost-benefit function η of an allele with its fixation probability.
515 First, we assume that each protein encoded within a genome provides some beneficial function and that
516 the organism needs that functionality to be produced at a target average rate ψ . Again, by definition,
517 the optimal amino acid sequence for a given gene, \vec{a}^* , produces one unit of functionality, i.e. $\mathbf{B}(\vec{a}^*) = 1$.
518 Second, we assume that the actual average rate a protein is synthesized ϕ is regulated by the organism
519 to ensure that functionality is produced at rate ψ . As a result, it follows that $\phi = \psi / \mathbf{B}(\vec{a} | \vec{a}^*)$ and the
520 energetic burden of a suboptimal amino acid increases the more it decreases the protein's functionality,

B. In other words, the average production rate of a protein \vec{a} with relative functionality $\mathbf{B}(\vec{a}) < 1$ must be $1/\mathbf{B}(\vec{a}|\vec{a}^*)$ times higher than the production rate needed if the optimal amino acid sequence \vec{a}^* was encoded since $\mathbf{B}(\vec{a}^*|\vec{a}^*)=1$. For example, a cell with an allele \vec{a} where $\mathbf{B}(\vec{a}|\vec{a}^*)=9/10$ would have to produce the protein at rate $\phi=10/9 \times \psi=1.11\psi$. Similarly, a cell with an allele \vec{a} where $\mathbf{B}(\vec{a}|\vec{a}^*)=1/2$ will have to produce the protein at $\phi=2\psi$. In contrast, a cell with the optimal allele \vec{a}^* would have to produce the protein at rate $\phi=\psi$.

Third, we assume that every additional high energy phosphate bond, $\sim P$, spent per unit time to meet the organism's target function synthesis rate ψ leads to a slight and proportional decrease in fitness W . This assumption, in turn, implies

$$W_i(\vec{c}) \propto \exp[-A_0 \eta(\vec{c}_i) \psi].$$

where A_0 , again, describes the proportional decline in fitness with every $\sim P$ wasted per unit time. Because A_0 shares the same time units as ψ and ϕ and only occurs in SelAC in conjunction with ψ , we do not need to explicitly identify our time units. Instead, we recognize that our estimates of ψ share an unknown scaling term.

Correspondingly, the ratio of fitness between two genotypes is,

$$\begin{aligned} W_i/W_j &= \exp[-A_0 \eta(\vec{c}_i) \psi] / \exp[-A_0 \eta(\vec{c}_j) \psi] \\ &= \exp[-A_0 (\eta(\vec{c}_i) - \eta(\vec{c}_j)) \psi] \end{aligned}$$

Given our formulations of **C** and **B**, the fitness effects between sites are multiplicative and, therefore, the substitution of an amino acid at one site can be modeled independently of the amino acids at the other sites within the coding sequence. As a result, the fitness ratio for two genotypes differing at multiple sites simplifies to

$$W_i/W_j = \exp \left[- \left(\frac{A_0 (A_1 + A_2 n_g)}{n_g} \right) \sum_{p \in \mathbb{P}} [d(a_{i,p}, a_p^*) - d(a_{j,p}, a_p^*)] G_p \psi \right]$$

where \mathbb{P} represents the codon positions in which \vec{c}_i and \vec{c}_j differ. Fourth, we make a weak mutation assumption, such that alleles can differ at only one position at any given time, i.e. $|\mathbb{P}|=1$, and that the population is evolving according to a Wright-Fisher process. As a result, the probability a new mutant, j , introduced via mutation into a resident population i with effective size N_e will go to fixation is,

$$\begin{aligned} u_{i,j} &= \frac{1 - (W_i/W_j)^b}{1 - (W_i/W_j)^{2N_e}} \\ &= \frac{1 - \exp \left\{ - \frac{A_0}{n_g} (A_1 + A_2 n_g) [d(a_i, a^*) - d(a_j, a^*)] G_p \psi b \right\}}{1 - \exp \left\{ - \frac{A_0}{n_g} (A_1 + A_2 n_g) [d(a_i, a^*) - d(a_j, a^*)] G_p \psi 2N_e \right\}} \end{aligned}$$

where $b=1$ for a diploid population and 2 for a haploid population (?????). Finally, assuming a constant mutation rate between alleles i and j , $\mu_{i,j}$, the substitution rate from allele i to j can be modeled as,

$$q_{i,j} = \frac{2}{b} \mu_{i,j} N_e u_{i,j}.$$

where, given the substitution model's weak mutation assumption, $N_e \mu \ll 1$. In the end, each optimal amino acid has a separate 61×61 substitution rate matrix \mathbf{Q}_a , which incorporates selection for the amino acid (and the fixation rate matrix this creates) as well as the common mutation parameters across optimal amino acids. This results in the creation of 20 \mathbf{Q} matrices, one for each amino acid and each with 3,721 entries which are based on a relatively small number of model parameters (one to 11 mutation rates, two free Grantham weights, the cost of protein assembly, A_1 and A_2 , the gene specific target functionality synthesis rate ψ , and optimal amino acid at each position p , a_p^*). These model parameters can either be specified *a priori* and/or estimated from the data.

Given our assumption of independent evolution among sites, it follows that the probability of the whole data set is the product of the probabilities of observing the data at each individual site. Thus, the likelihood \mathcal{L} of amino acid a being optimal at a given site position p is calculated as

$$\mathcal{L}(\mathbf{Q}_a | \mathbf{D}_p, \mathbf{T}) \propto \mathbf{P}(\mathbf{D}_p | \mathbf{Q}_a, \mathbf{T}) \quad (2)$$

In this case, the data, \mathbf{D}_p , are the observed codon states at position p for the tips of the phylogenetic tree with topology \mathbf{T} . For our purposes we take \mathbf{T} as given, but it could be estimated as well. The pruning algorithm of ? is used to calculate $\mathcal{L}(\mathbf{Q}_a | \mathbf{D}_p, \mathbf{T})$. The log of the likelihood is maximized by estimating the genome scale parameters which consist of 11 mutation parameters, which are implicitly scaled by $2N_e/b$, and two Grantham distance parameters, α_c and α_p , and the sensitivity distribution parameter α_G . Because A_0 and ψ_g always co-occur and are scaled by N_e , for each gene g we estimate a composite term $\psi'_g = \psi_g A_0 b N_e$ and the optimal amino acid for each position a_p^* of the protein. When estimating α_G , the likelihood then becomes the average likelihood which we calculate using the generalized Laguerre quadrature with $k=4$ points (?).

Finally, we note that because we infer the ancestral state of the system, our approach does not rely on any assumptions of model stationarity. Nevertheless, as our branch lengths grow the probability of observing a particular amino acid a at a given site approaches a stationary value proportional to $W(a)^{2N_e-b}$ and any effects of mutation bias (?).

Implementation

All methods described above are implemented in the new R package, `selac` available through GitHub (<https://github.com/bomeara/selac>) which will be uploaded to CRAN once peer review has

572 completed. Our package requires as input a set of fasta files that each contain an alignment of coding
573 sequence for a set of taxa, and the phylogeny depicting the hypothesized relationships among them. In
574 addition to the SelAC models, we implemented the GY codon model of ?, the FMutSel mutation-selection
575 model of ?, and the standard general time-reversible nucleotide model that allows for Γ distributed rates
576 across sites. These likelihood-based models represent a sample of the types of popular models often fit
577 to codon data.

578 For the SelAC models, the starting guess for the optimal amino acid at a site comes from ‘majority’
579 rule, where the initial optimum is the most frequently observed amino acid at a given site (ties resolved
580 randomly). Our optimization routine utilizes a four stage hill climbing approach. More specifically, within
581 each stage a block of parameters are optimized while the remaining parameters are held constant. The
582 first stage optimizes the block of branch length parameters. The second stage optimizes the block of
583 gene specific composite parameters $\psi'_g = A_0 \psi_g N_e b$. The third stage optimizes SelAC’s parameters shared
584 across the genome α_c and α_p , and the sensitivity distribution parameter α_G . The fourth stage estimates
585 the optimal amino acid at each site a^* . This entire four stage cycle is repeated six more times, using
586 the estimates from the previous cycle as the initial conditions for the new one. The search is terminated
587 when the improvement in the log-likelihood between cycles is less than 10^{-8} at which point we consider
588 the ML solution found and the search is terminated. For optimization of a given set of parameters, we
589 rely on a bounded subplex routine (?) in the package NLOptR (?) to maximize the log-likelihood function.
590 To ensure the robustness of our results, we perform a set of independent analyses with different sets of
591 naive starting points with respect to the gene specific composite ψ' parameters, α_c , and α_p and were
592 able to repeatedly reach the same log-likelihood (lnL) peak in our parameter space. Confidence in the
593 parameter estimates can be generated by an ‘adaptive search’ procedure that we implemented to provide
594 an estimate of the parameter space that is some pre-defined likelihood distance (e.g., 2 lnL units) from
595 the maximum likelihood estimate (MLE), which follows ? and ?.

596 We note that our current implementation of SelAC is slow, and is best suited for data sets with relatively
597 small number of taxa (i.e. 10’s not 100’s). This limitation is largely due to the size and quantity of matrices
598 we create and manipulate to calculate the log-likelihood of an individual site. Ongoing work will address
599 the need for speed, with the eventual goal of implementing SelAC in popular phylogenetic inference
600 toolkits, such as RevBayes (?), PAML (?) and RAxML (?).

601 Simulations

602 We evaluated the performance of our codon model by simulating datasets and estimating the bias of
603 the inferred model parameters from these data. Our ‘known’ parameters under a given generating model

were based on fitting SelAC to the 106 gene data set and phylogeny of ?. The tree used in these analyses is outdated with respect to the current hypothesis of relationships within *Saccharomyces*, but we rely on it simply as a training set that is separate from our empirical analyses (see section below). Bias in the model parameters were assessed under two generating models: one where we assumed a model of SelAC assuming uniform sensitivity across sites (i.e. $G_p=1$ for all sites, i.e. $\alpha_G=\infty$), and one where we used the Gamma distribution joint shape and rate parameter α_G estimated from the empirical data. Under each of these two scenarios, we used parameter estimates from the corresponding empirical analysis and simulated 50 five-gene data sets. For the gene specific composite parameter ψ'_g the ‘known’ values used for the simulation were five evenly spaced points along the rank order of the estimates across the 106 genes. The MLE estimate for a given replicate were taken as the fit with the highest log-likelihood after running five independent analyses with different sets of naive starting points with respect to the composite ψ'_g parameter, α_c , and α_p . All analyses were carried out in our `selac` R package.

Analysis of yeast genomes & tests of model adequacy

We focus our empirical analyses on the large yeast data set and phylogeny of ?. As a model system, the yeast genome is an ideal system to examine our phylogenetic estimates of gene expression and its connection to real world measurements of these data within individual taxa. The complete data set of ? contain 1070 orthologs, where we selected 100 at random for our analyses. We also focus our analyses on *Saccharomyces sensu stricto* and their sister taxon *Candida glabrata*, and we used the phylogeny depicted in Fig. 1 of ? for our fixed tree. We fit the two SelAC models described above (i.e., SelAC and SelAC+ Γ), as well as two codon models, GY and FMutSel, and a standard GTR + Γ nucleotide model. The FMutSel model assumes that the amino acid frequencies are determined by functional requirements of the protein while the other models make no assumptions about amino acid frequencies. In all cases, we assumed that the model was partitioned by gene, but with branch lengths linked across genes.

We also compared SelAC models with 195 codon models in IQtree (?). This is popular software implementing various (i.e., ????) models of evolution, including codon models. Most analyses within a set of software tools focus on differences in log-likelihood values between models. As a result, some software tools sometimes fail to include solely data dependent terms, which function as constants, in their calculations. Failure to include these terms can model comparison between software packages problematic. For simplicity, no constants are dropped in the log-likelihood calculations for SelAC. Further, while there are no identical models in SelAC and IQtree, similar models have similar likelihoods, suggesting the log-likelihood values between SelAC and IQtree are comparable (as one would expect). We note, however, that minor differences in model implementation can lead to small differences in log likelihood (for example,

636 how missing data is handled, as SelAC treats it as an absence at that site for that taxon, while some
637 other software integrates across all possible states).

638 For SelAC, we compared our estimates of $\phi' = \psi' / \mathbf{B}$, which represents the average protein synthesis
639 rate of a gene, to estimates of gene expression from empirical data. Specifically, we examined gene
640 expression data for five of the six species measured during log-growth phase. Gene expression in this
641 context corresponds to mRNA abundances, which were measured using either microarrays (*C. glabrata*
642 and *S. castellii*, or RNA-Seq (*S. paradoxus*, *S. mikatae*, and *S. cerevisiae*). We obtained expression data
643 for the remaining species, *S. kudriavzevii*, which was measured at the beginning of the stationary phase
644 from the Gene Expression Omnibus (GEO). *Saccharomyces*, however, only enter the stationary growth
645 phase in response to severe stress, such as starvation. In addition, only 56 % of the genes examined with
646 SelAC had expression measurements available. For these reasons, we excluded *S. kudriavzevii* from our
647 comparisons of empirical gene expression.

648 For further comparison, we also predicted the average protein synthesis rate for each gene ϕ by
649 analyzing gene and genome-wide patterns of synonymous codon usage using ROC-SEMPPR (?) for
650 each individual genome. While, like SelAC, ROC-SEMPPR uses codon level information, it does not
651 rely on any interspecific comparisons and, unlike SelAC, uses only the intra- and inter-genic frequencies
652 of synonymous codon usage as its data. Nevertheless, ROC-SEMPPR predictions of gene expression
653 ϕ correlates strongly (Pearson $r = 0.53 - 0.74$) with a wide range of laboratory measurements of gene
654 expression (?).

655 While one of our main objectives was to determine the improvement of fit that SelAC has with respect
656 to other standard phylogenetic models, we also evaluated the adequacy of SelAC. Model fit, measured
657 with assessments such as the Akaike Information Criterion (AIC), can tell which model is least bad as
658 an approximation for the data, but it does not reveal whether a model is actually doing a good job of
659 representing the data. An adequate model does the latter, one measure of which is that data generated
660 under the model resemble real data (?). For example, ? assessed whether parsimony scores and the size
661 of monomorphic clades of empirical data were within the distributions of simulated data under a new
662 model and the best standard model; if the empirical summaries were outside the range for each, it would
663 have suggested that neither model was adequately modeling this part of the biology.

664 In order to test adequacy for a given gene we first remove a particular taxon from the data set
665 and the phylogeny. A marginal reconstruction of the likeliest sequence across all remaining nodes is
666 conducted under the model, including the node where the pruned taxon attached to the tree. The
667 marginal probabilities of each site are used to sample and assemble the starting coding sequence. This

sequence is then evolved along the branch, periodically being sampled and its current functionality assessed. We repeat this process 100 times and compare the distribution of trajectories against the observed functionality calculated for the gene. For comparison, we also conducted the same test, by simulating the sequence under the standard GTR + Γ nucleotide model, which is often used on these data but does not account for the fact that the sequences are protein coding, and under FMutSel, which includes selection on codons but in a fundamentally different way as our model.

The appropriate estimator of bias for AIC

As part of the model set described above, we also included a reduced form of each of the two SelAC models, SelAC and SelAC+ Γ . Specifically, rather than optimizing the amino acid at any given site, we assume the the most frequently observed amino acid at each site is the optimal amino acid a^* . We refer to these ‘majority rule’ models as SelAC_M and SelAC_M+ Γ and note that these majority rule formulations greatly accelerate model fitting.

Since these majority rule models assume that the optimal amino acids are known prior to fitting of our model, it is tempting to reduce the count of estimated parameters in the model by the number of parameters estimated using majority rule. While using majority rule does not necessarily provide the most likely parameter estimate, it nevertheless uses the data to generate the estimate and represents a parameter estimated from the data. Thus, despite having become standard behavior in the field of phylogenetics, this reduction is statistically inappropriate. Because the difference in the number of parameters K when counting or not counting the number of nucleotide sites drops out when comparing nucleotide models with AIC, this statistical issue does not apply to nucleotide models. It does, however, matter for AICc, where K and the sample size n combine in the penalty term. This also matters in our case, where the number of estimated parameters for the majority rule estimation differs based on whether one is looking at codons or single nucleotides.

In phylogenetics two variants of AICc are used. In comparative methods (e.g. ???) the number of data points, n , is taken as the number of taxa. More taxa allow the fitting of more complex models, given more data. However, in DNA evolution, which is effectively the same as a discrete character model used in comparative methods, the n is taken as the number of sites. Obviously, both cannot be correct. This uncertainty was highlighted by ?: they chose to use number of sites, but mentioned in their discussion that sample size also depends on the number of taxa. ? also mention that while the number of sites is often taken as sample size, whether that is appropriate in phylogenetics is not entirely clear. One approach incorporating both number of taxa and sites in calculating AICc is the program SURFACE implemented by ?, which uses multiple characters and taxa. While its default is to use AIC to compare

models, if one chooses to use AICc, the number of samples is taken as the product of number of sites and number of taxa.

Recently, ? performed an analysis that investigated what variant of AIC and AICc worked best as an estimator, but the results were inconclusive. Here, we have adopted and extended the simulation approach of ? in order to examine a large set of different penalty functions and how well they approximate the remaining portion of the Kullback-Liebler (KL) divergence between two models after accounting for the deviance (i.e., $-2\mathcal{L}$) (see Appendix 1 for more details).

Acknowledgements

This work was supported in part by NSF Awards MCB-1120370 (MAG and RZ) and DEB-1355033 (BCO, MAG, and RZ) with additional support from The University of Tennessee Knoxville and University of Arkansas (JMB). JJC and JMB received support as Postdoctoral Fellows and CL received support as a Graduate Student Fellow at the National Institute for Mathematical and Biological Synthesis, an Institute sponsored by the National Science Foundation through NSF Award DBI-1300426, with additional support from UTK. The authors would like to thank Premal Shah, Todd Oakley, and four anonymous reviewers for their helpful criticisms and suggestions for this work.

References

- Allison, S. 2012. A trait-based approach for modelling microbial litter decomposition. *Ecology Letters*, 15: 1058–1070.
- Allison, S. and Goulden, M. 2017. Consequences of drought tolerance traits for microbial decomposition in the dement model. *Soil Biology & Biochemistry*, 107: 104–113.
- Anisimova, M. 2012. Parametric models of codon evolution. In G. M. Cannarozzi and A. Schneider, editors, *Codon Evolution: Mechanisms and Models*, pages 12–33. Oxford University Press, Oxford, UK.
- Asimov, I. 1989. The relativity of wrong. *The Skeptical Inquirer*, 14(1): 35–44.
- Beaulieu, J. M. and O’Meara, B. C. 2016. Detecting hidden diversification shifts in models of trait-dependent speciation and extinction. *Systematic Biology*, 65(4): 583–601.
- Beaulieu, J. M., O’Meara, B. C., and Donoghue, M. J. 2013. Identifying hidden rate changes in the evolution of a binary morphological character: The evolution of plant habit in campanulid angiosperms. *Systematic Biology*, 62(5): 725–737.
- Berg, J. and Lässig, M. 2003. Stochastic evolution and transcription factor binding sites. *Biophysics*, 48(S1): S36–S44.
- Błażej, P., Mackiewicz, D., Grabińska, M., Wnetrzak, M., and Mackiewicz, P. 2017. Optimization of amino acid replacement costs by mutational pressure in bacterial genomes. *Scientific Reports*, 7(1): 1061.
- Box, G. E. P. 1976. Science and statistics. *Journal of the American Statistical Association*, 71(356): 791–799.
- Brown, L. and Elliot, T. 1997. Mutations that increase expression of the rpos gene and decrease its dependence on hfq function in salmonella typhimurium. *J. Bacteriol.*, 179(3): 656–662.
- Butler, M. A. and King, A. A. 2004. Phylogenetic comparative analysis: a modeling approach for adaptive evolution. *American Naturalist*, 164(6): 683–695.
- Dimmic, M. W., Mindell, D. P., and Goldstein, R. A. 2000. Modeling evolution at the protein level using an adjustable amino acid fitness model. *Pacific Symposium on Biocomputing*, 5: 18–29.
- Drummond, D. A. and Wilke, C. O. 2008. Mistranslation-induced protein misfolding as a dominant constraint on coding-sequence evolution. *Cell*, 134: 341–352.
- Drummond, D. A., Bloom, J. D., Adami, C., Wilke, C. O., and Arnold, F. H. 2005. Why highly expressed proteins evolve slowly. *Proceedings of the National Academy of Sciences of the United States of America*, 102(40): 14338–14343.
- Drummond, D. A., Raval, A., and Wilke, C. O. 2006. A single determinant dominates the rate of yeast protein evolution. *Molecular Biology and Evolution*, 23(2): 327–337.
- Edwards, A. 1984. *Likelihood*. Cambridge science classics. Cambridge University Press.
- Endler, J. A. 1986. *Natural Selection in the Wild*, pages 16–17. Number 21 in Monographs in Population Biology. Princeton University Press, Princeton, NJ. reference for definition of diversifying selection.
- Felsenstein, J. 1981. Evolutionary trees from DNA-sequences - a maximum-likelihood approach. *Journal of Molecular Evolution*, 17: 368–376.
- Felsenstein, J. 2001. Taking variation of evolutionary rates between sites into account in inferring phylogenies. *Journal of Molecular Evolution*, 53(4): 447–455.
- Fisher, Ronald A., S. 1930. *The Genetical Theory of Natural Selection*. Oxford University Press, Oxford.
- Gilchrist, M., Shah, P., and Zaretzki, R. 2009. Measuring and detecting molecular adaptation in codon usage against nonsense errors during protein translation. *Genetics*, 183: 1493–1505.

752 Gilchrist, M. A. 2007. Combining models of protein translation and population genetics to predict protein production rates
 753 from codon usage patterns. *Molecular Biology and Evolution*, 24: 2362–2373.
 754 Gilchrist, M. A. and Wagner, A. 2006. A model of protein translation including codon bias, nonsense errors, and ribosome
 755 recycling. *Journal of Theoretical Biology*, 239: 417–434.
 756 Gilchrist, M. A., Chen, W.-C., Shah, P., Landerer, C. L., and Zaretzki, R. 2015. Estimating gene expression and codon-
 757 specific translational efficiencies, mutation biases, and selection coefficients from genomic data alone. *Genome Biology
 758 and Evolution*, 7(6): 1559–1579.
 759 Goldman, N. 1993. Statistical tests of models of dna substitution. *Journal of molecular evolution*, 36(2): 182–198.
 760 Goldman, N. and Yang, Z. H. 1994. Codon-based model of nucleotide substitution for protein-coding DNA-sequences.
 761 *Molecular Biology and Evolution*, 11: 725–736.
 762 Goldman, N., Thorne, J. L., and Jones, D. T. 1996. Using evolutionary trees in protein secondary structure prediction and
 763 other comparative sequence analyses. *Journal of Molecular Biology*, 263(2): 196 – 208.
 764 Goldman, N., Thorne, J. L., and Jones, D. T. 1998. Assessing the impact of secondary structure and solvent accessibility
 765 on protein evolution. *Genetics*, 149(1): 445–458.
 766 Goldsmith, M. and Tawfik, D. S. 2009. Potential role of phenotypic mutations in the evolution of protein expression and
 767 stability. *Proceedings of the National Academy of Sciences*, 106(15): 6197–6202.
 768 Grantham, R. 1974. Amino acid difference formula to help explain protein evolution. *Science*, 185(4154): 862–864.
 769 Halpern, A. L. and Bruno, W. J. 1998. Evolutionary distances for protein-coding sequences: Modeling site-specific residue
 770 frequencies. *Molecular Biology And Evolution*, 15: 910–917.
 771 Higgs, P. G. 2008. Linking population genetics to phylogenetics. *Banach Center Publications*, 80(1): 145–166.
 772 Hoehna, S., Landis, M. J., Heath, T. A., Boussau, B., Lartillot, N., Moore, B. R., Huelsenbeck, J. P., and Ronquist, F.
 773 2016. Revbayes: Bayesian phylogenetic inference using graphical models and an interactive model-specification language.
 774 *Systematic Biology*, 65(4): 726.
 775 Hughes, A. L. 2007. Looking for darwin in all the wrong places: the misguided quest for positive selection at the nucleotide
 776 sequence level. *Heredity*, 99: 364–373.
 777 Hughes, A. L. and Nei, M. 1988. Pattern of nucleotide substitution at major histocompatibility complex class-i loci reveals
 778 overdominant selection. *Nature*, 335: 167–170.
 779 Hughes, A. L., Ota, T., and Nei, M. 1990. Positive darwinian selection promotes charge profile diversity in the antigen-binding
 780 cleft of class-i major-histocompatibility-complex molecules. *Molecular Biology And Evolution*, 7: 515–524.
 781 Ingram, T. and Mahler, D. L. 2013. Surface: detecting convergent evolution from data by fitting ornstein-uhlenbeck models
 782 with stepwise akaike information criterion. *Methods in ecology and evolution*, 4(5): 416–425.
 783 Iwasa, Y. 1988. Free fitness that always increases in evolution. *Journal of Theoretical Biology*, 135: 265–281.
 784 Jhwueng, D.-C., Snehata, H., O’Meara, B. C., and Liu, L. 2014. Investigating the performance of aic in selecting
 785 phylogenetic models. *Statistical applications in genetics and moleculr biology*, 13(4): 459–475.
 786 Johnson, S. G. 2012. *The NLOpt nonlinear-optimization package*. Version 2.4.2 – Released 20 May 2014.
 787 Kimura, M. 1962. on the probability of fixation of mutant genes in a population. *Genetics*, 47(6): 713–719.
 788 King, Z. A., Lloyd, C. J., Feist, A. M., and Palsson, B. O. 2015. Next-generation genome-scale models for metabolic
 789 engineering. *Current Opinion in Biotechnology*, 35: 23 – 29.

- 790 Koshi, J. M. and Goldstein, R. A. 1997. Mutation matrices and physical-chemical properties: Correlations and implications.
791 *Proteins-Structure Function And Genetics*, 27: 336–344.
- 792 Koshi, J. M. and Goldstein, R. A. 2000. Analyzing site heterogeneity during protein evolution. In *Biocomputing 2001*, pages
793 191–202. World Scientific.
- 794 Koshi, J. M., Mindell, D. P., and Goldstein, R. A. 1999. Using physical-chemistry-based substitution models in phylogenetic
795 analyses of hiv-1 subtypes. *Molecular biology and evolution*, 16: 173–179.
- 796 Kosiol, C., Holmes, I., and Goldman, N. 2007. An empirical codon model for protein sequence evolution. *Molecular Biology
797 and Evolution*, 24(7): 1464–1479.
- 798 Kubatko, L., Shah, P., Herbei, R., and Gilchrist, M. A. 2016. A codon model of nucleotide substitution with selection on
799 synonymous codon usage. *Molecular Phylogenetics and Evolution*, 94(Part A): 290 – 297.
- 800 Lartillot, N. and Philippe, H. 2004. A bayesian mixture model for across-site heterogeneities in the amino-acid replacement
801 process. *Molecular Biology And Evolution*, 21: 1095–1109.
- 802 Lerman, J. A., Hyduke, D. R., Latif, H., Portnoy, V. A., Lewis, N. E., Orth, J. D., Schrimpe-Rutledge, A. C., Smith,
803 R. D., Adkins, J. N., Zengler, K., and Palsson, B. O. 2012. In silico method for modelling metabolism and gene product
804 expression at genome scale. *Nature Communications*, 3: 929 EP –. Article.
- 805 Lynch, M. and Marinov, G. K. 2015. The bioenergetic costs of a gene. *Proceedings Of The National Academy Of Sciences
806 Of The United States Of America*, 112: 15690–15695.
- 807 Mayrose, I., Friedman, N., and Pupko, T. 2005. A gamma mixture model better accounts for among site rate heterogeneity.
808 *Bioinformatics*, 21(suppl-2): ii151–ii158.
- 809 McCandlish, D. M. and Stoltzfus, A. 2014. Modeling evolution using the probability of fixation: History and implications.
810 *The Quarterly Review of Biology*, 89(3): 225–252.
- 811 McClellan, D. A. and McCracken, K. G. 2001. Estimating the influence of selection on the variable amino acid sites of the
812 cytochrome b protein functional domains. *Molecular Biology And Evolution*, 18: 917–925.
- 813 Muse, S. V. and Gaut, B. S. 1994. A likelihood approach for comparing synonymous and nonsynonymous nucleotide
814 substitution rates, with application to the chloroplast genome. *Molecular Biology and Evolution*, 11(5): 715–724.
- 815 Nguyen, L.-T., Schmidt, H. A., von Haeseler, A., and Minh, B. Q. 2015. Iq-tree: A fast and effective stochastic algorithm
816 for estimating maximum-likelihood phylogenies. *Molecular Biology and Evolution*, 32(1): 268–274.
- 817 Nielsen, R. and Yang, Z. H. 1998. Likelihood models for detecting positively selected amino acid sites and applications to
818 the hiv-1 envelope gene. *Genetics*, 148: 929–936.
- 819 Nowak, M. A. 2006. *Evolutionary Dynamics: Exploring the Equations of Life*. Belknap of Harvard University Press,
820 Cambridge, MA.
- 821 O’Meara, B. C., Ane, C., Sanderson, M. J., and P.C., W. 2006. Testing for different rates of continuous trait evolution using
822 likelihood. *Evolution*, 60(5): 922–933.
- 823 Pellmyr, O. 2002. Microevolution. In M. Pagel, editor, *Encyclopedia of Evolution*, volume 2, pages 731–732. Oxford
824 University Press, Oxford, UK.
- 825 Penny, D., McComish, B. J., Charleston, M. A., and Hendy, M. D. 2001. Mathematical elegance with biochemical realism:
826 The covarion model of molecular evolution. *Journal Of Molecular Evolution*, 53: 711–723.
- 827 Pollock, D. D., Thiltgen, G., and Goldstein, R. A. 2012. Amino acid coevolution induces an evolutionary stokes shift.
828 *Proceedings Of The National Academy Of Sciences Of The United States Of America*, 109: E1352–E1359.

829 Posada, D. and Buckley, T. R. 2004. Model selection and model averaging in phylogenetics: advantages of akaike information
830 criterion and bayesian approaches over likelihood ratio tests. *Systematic Biology*, 53(5): 793–808.

831 Pouyet, F., Bailly-Bechet, M., Mouchiroud, D., and Guguen, L. 2016. Senca: A multilayered codon model to study the
832 origins and dynamics of codon usage. *Genome Biology and Evolution*, 8(8): 2427–2441.

833 Robinson, D. M., Jones, D. T., Kishino, H., Goldman, N., and Thorne, J. L. 2003. Protein evolution with dependence among
834 codons due to tertiary structure. *Molecular Biology And Evolution*, 20: 1692–1704.

835 Rodrigue, N. and Lartillot, N. 2014. Site-heterogeneous mutation-selection models within the phylobayes-mpi package.
836 *Bioinformatics*, 30: 1020–1021.

837 Rodrigue, N., Lartillot, N., Bryant, D., and Philippe, H. 2005. Site interdependence attributed to tertiary structure in amino
838 acid sequence evolution. *Gene*, 347: 207–217.

839 Rokas, A., Williams, B. L., King, N., and Carroll, S. B. 2003. Genome-scale approaches to resolving incongruence in
840 molecular phylogenies. *Nature*, 425: 798–804.

841 Rowan, T. 1990. *Functional Stability Analysis of Numerical Algorithms*. Ph.D. thesis, University of Texas, Austin.

842 Salichos, L. and Rokas, A. 2013. Inferring ancient divergences requires genes with strong phylogenetic signals. *Nature*,
843 497(7449): 327–331.

844 Sella, G. and Hirsh, A. E. 2005. The application of statistical physics to evolutionary biology. *Proceedings of the National*
845 *Academy of Sciences of the United States of America*, 102: 9541–9546.

846 Shah, P. and Gilchrist, M. A. 2011. Explaining complex codon usage patterns with selection for translational efficiency,
847 mutation bias, and genetic drift. *Proceedings of the National Academy of Sciences of the United States of America*,
848 108(25): 10231–10236.

849 Shah, P., McCandlish, D. M., and Plotkin, J. B. 2015. Contingency and entrenchment in protein evolution under purifying
850 selection. *Proceedings of the National Academy of Sciences*, 112(25): E3226–E3235.

851 Stamatakis, A. 2006. RAxML-VI-HPC: maximum likelihood-based phylogenetic analyses with thousands of taxa and mixed
852 models. *Bioinformatics*, 22(21): 2688–2690.

853 Sullivan, J. and Joyce, P. 2005. Model selection in phylogenetics. *Annual Review of Ecology, Evolution, and Systematics*,
854 36(1): 445–466.

855 Tamuri, A. U., dos Reis, M., Hay, A. J., and Goldstein, R. A. 2009. Identifying changes in selective constraints: Host shifts
856 in influenza. *Plos Computational Biology*, 5.

857 Tamuri, A. U., dos Reis, M., and Goldstein, R. A. 2012. Estimating the distribution of selection coefficients from phylogenetic
858 data using sitewise mutation-selection models. *Genetics*, 190: 1101–1115.

859 Tamuri, A. U., Goldman, N., and dos Reis, M. 2014. A penalized-likelihood method to estimate the distribution of selection
860 coefficients from phylogenetic data. *Genetics*, 197: 257–271.

861 Thiele, I., Fleming, R. M. T., Que, R., Bordbar, A., Diep, D., and Palsson, B. O. 2012. Multiscale modeling of metabolism
862 and macromolecular synthesis in e. coli and its application to the evolution of codon usage. *PLOS ONE*, 7(9): 1–18.

863 Thorne, J. L., Goldman, N., and Jones, D. T. 1996. Combining protein evolution and secondary structure. *Molecular Biology*
864 *and Evolution*, 13(5): 666–673.

865 Thorne, J. L., Lartillot, N., Rodrigue, N., and Choi, S. C. 2012. Codon models as a vehicle for reconciling
866 population genetics with inter-specific sequence data. *Codon Evolution: Mechanisms And Models*, pages 97–110 D2
867 10.1093/acprof:osobl/9780199601165.001.0001 ER.

- 868 Tuffley, C. and Steel, M. 1998. Modeling the covarion hypothesis of nucleotide substitution. *Mathematical Biosciences*, 147:
869 63–91.
- 870 Wagner, A. 2005. Energy constraints on the evolution of gene expression. *Molecular Biology and Evolution*, 22: 1365–1374.
- 871 Whelan, S. 2008. The genetic code can cause systematic bias in simple phylogenetic models. *Philosophical Transactions Of*
872 *The Royal Society B-Biological Sciences*, 363: 4003–4011.
- 873 Whelan, S. and Goldman, N. 2004. Estimating the frequency of events that cause multiple-nucleotide changes. *Genetics*,
874 167(4): 2027–2043.
- 875 Woolley, S., Johnson, J., Smith, M. J., Crandall, K. A., and McClellan, D. A. 2003. Treesaap: Selection on amino acid
876 properties using phylogenetic trees. *Bioinformatics*, 19(5): 671–672.
- 877 Wright, S. 1969. *Evolution and the genetics of populations. Vol. 2. The theory of gene frequencies.*, volume 2. University of
878 Chicago Press.
- 879 Xia, X. H. and Li, W. H. 1998. What amino acid properties affect protein evolution? *Journal Of Molecular Evolution*, 47:
880 557–564.
- 881 Yang, Z. 2014. *Molecular Evolution: A Statistical Approach*. Oxford University Press, New York.
- 882 Yang, Z., Nielsen, R., and Hasegawa, M. 1998. Models of amino acid substitution and applications to mitochondrial protein
883 evolution. *Molecular Biology and Evolution*, 15: 1600–1611.
- 884 Yang, Z. H. 1994. Maximum-likelihood phylogenetic estimation from DNA-sequences with variable rates over sites -
885 approximate methods. *Journal Of Molecular Evolution*, 39: 306–314.
- 886 Yang, Z. H. 2007. Paml 4: Phylogenetic analysis by maximum likelihood. *Molecular Biology And Evolution*, 24: 1586–1591.
- 887 Yang, Z. H. and Nielsen, R. 1998. Synonymous and nonsynonymous rate variation in nuclear genes of mammals. *Journal*
888 *Of Molecular Evolution*, 46: 409–418.
- 889 Yang, Z. H. and Nielsen, R. 2008. Mutation-selection models of codon substitution and their use to estimate selective
890 strengths on codon usage. *Molecular Biology and Evolution*, 25: 568–579.
- 891 Zanger, U. and Schwab, M. 2013. Cytochrome p450 enzymes in drug metabolism: Regulation of gene expression, enzyme
892 activities, and impact of genetic variation. *Pharmacology & Therapeutics*, 138: 103–141.

Table

| Model | Parameters | | | | Model | |
|--------------------------------------|---------------------|-----------|-----------|-----------|---------------------|--------|
| | $-\ln(\mathcal{L})$ | Estimated | AIC | AICc | ΔAICc | Weight |
| SelAC+ Γ | 453,620.8 | 50,005 | 1,007,252 | 1,027,314 | 0 | >0.999 |
| SelAC | 464,114.8 | 50,004 | 1,028,238 | 1,048,299 | 20,985 | <0.001 |
| SelAC _{<i>M</i>} + Γ | 465,106.9 | 50,005 | 1,030,224 | 1,050,286 | 22,972 | <0.001 |
| SelAC _{<i>M</i>} | 478,302.4 | 50,004 | 1,056,613 | 1,076,674 | 49,360 | <0.001 |
| FMutSel | 597,140.7 | 178 | 1,194,637 | 1,194,638 | 167,324 | <0.001 |
| GY | 612,670.4 | 111 | 1,225,563 | 1,225,563 | 198,249 | <0.001 |
| GTR+ Γ | 655,166.4 | 610 | 1,311,553 | 1,311,554 | 284,240 | <0.001 |

Table 1. Comparison of maximum likelihood fits for SelAC and commonly used models based on negative log likelihood ($-\ln(\mathcal{L})$), AIC, AICc, and AIC_w from analyses of 100 selected genes from 6 yeast taxa. Note the subscripts *M* indicate model fits where the most common or ‘majority rule’ amino acid was fixed as the optimal amino acid a^* for each site. As discussed in text, despite the fact that a^* for each site under *M* was not fitted by our algorithm, its value was determined by examining the data and, as a result, represent an additional parameter estimated from the data and are accounted for in our table. Sample size used in the calculation of AICc is assumed to be equal to the size of the matrix (number of taxa \times number of sites = $6 \times 49,881 = 299,286$). For the comparison between the different SelAC and 192 other models fitted using IQTree (?) see Table ?? in the Supporting Materials. In summary, the different SelAC models and FMutSel fitted the data better than any of the IQTree models.

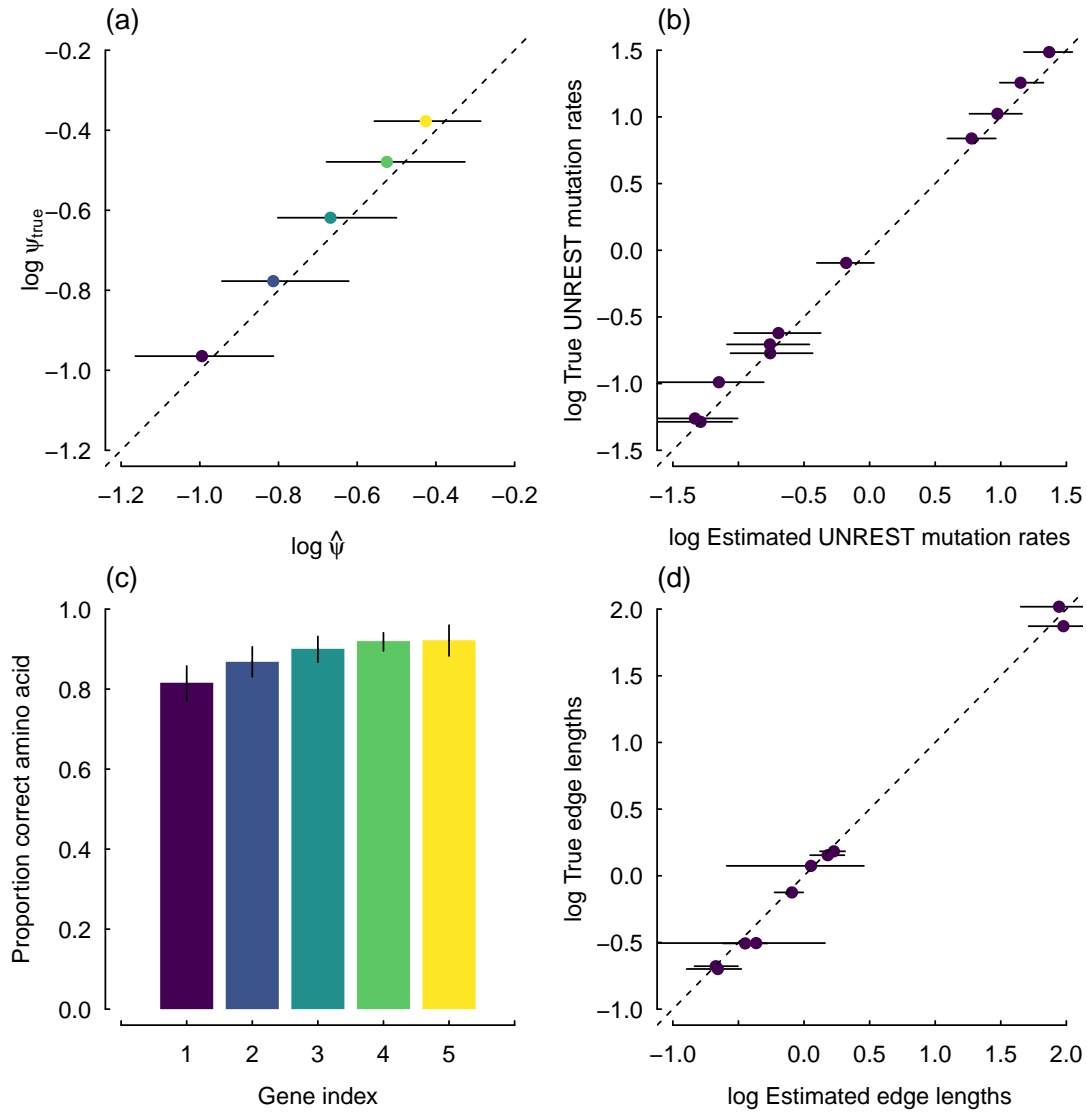


FIG. 1. Summary of a 5-gene simulation for a SelAC model where we assume $\alpha_G = \infty$, and thus, no site-specific sensitivity in the generating model. The ‘known’ parameters were based on fitting the SelAC model to the 106 gene data set and phylogeny of ?, with gene choice being based on five evenly spaced points along the rank order of the gene specific composite

parameter ψ'_g . The points and associated uncertainty in the estimates of the gene-specific average protein synthesis rate, or

ψ (calculated from ψ') (a), nucleotide mutation rates under the UNREST model (b), proportion of correct optimal amino acids for a given gene (c), and estimates of the individual edge lengths are based the mean and 2.5% and 97.5% quantiles across all 50 simulated datasets (d). Gene index on the x-axis refers to the arbitrary number assigned to the simulated gene.

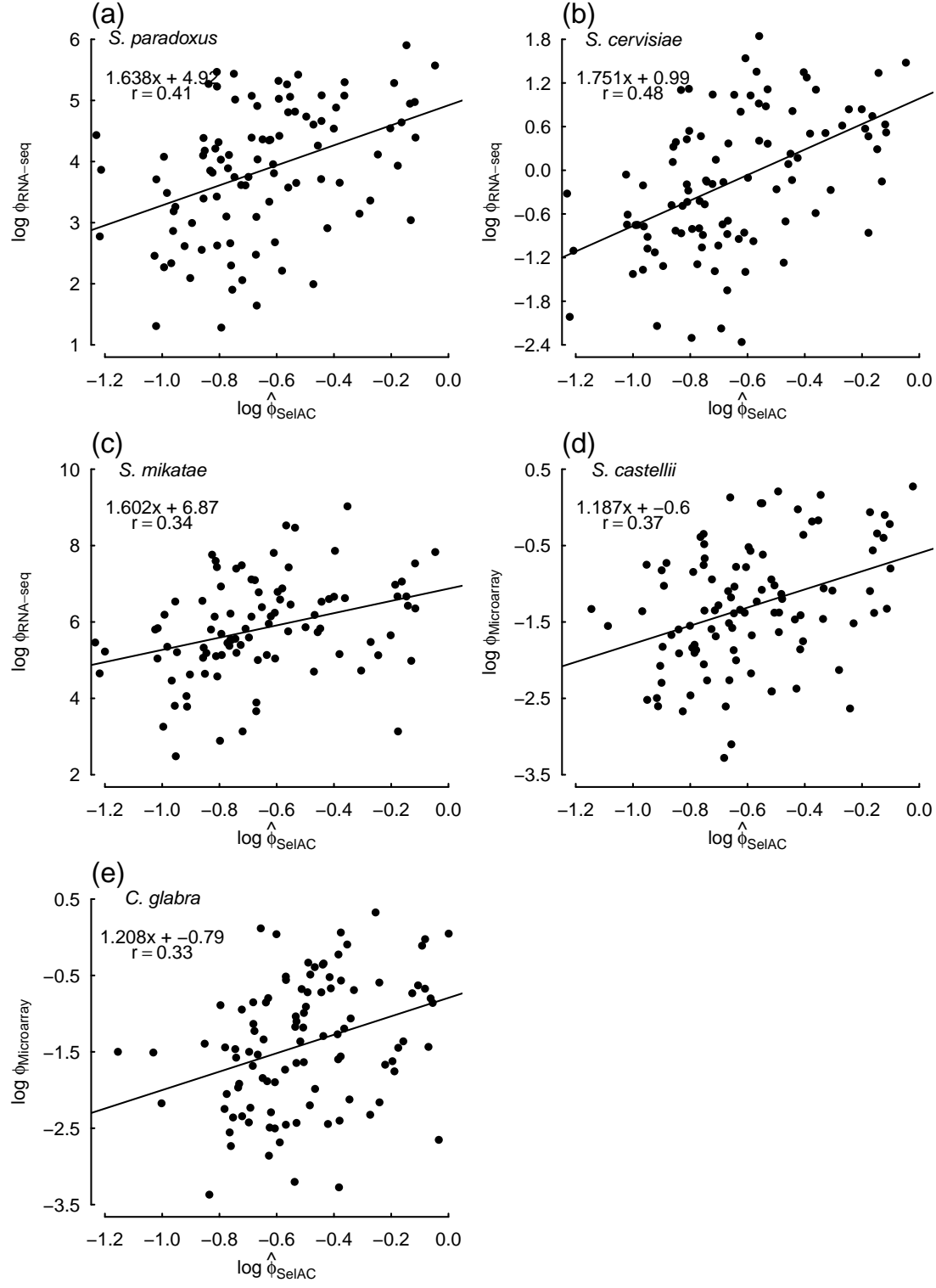


FIG. 2. Comparisons between estimates of average protein translation rate $\hat{\phi}_{\text{SelAC}}$ obtained from SelAC+ Γ and direct measurements of expression for individual yeast taxa across the 100 selected genes from ? measured during log-growth phase. Estimates of $\hat{\phi}_{\text{SelAC}}$ were generated by dividing the composite term ψ' by $\mathbf{B}(\vec{a}_i|\vec{a}^*)$. Gene expression was measured using either RNA-Seq (a)-(c) or microarray (d)-(e). The equations in the upper left hand corner of each panel represent the regression fit and the Pearson correlation coefficient r .

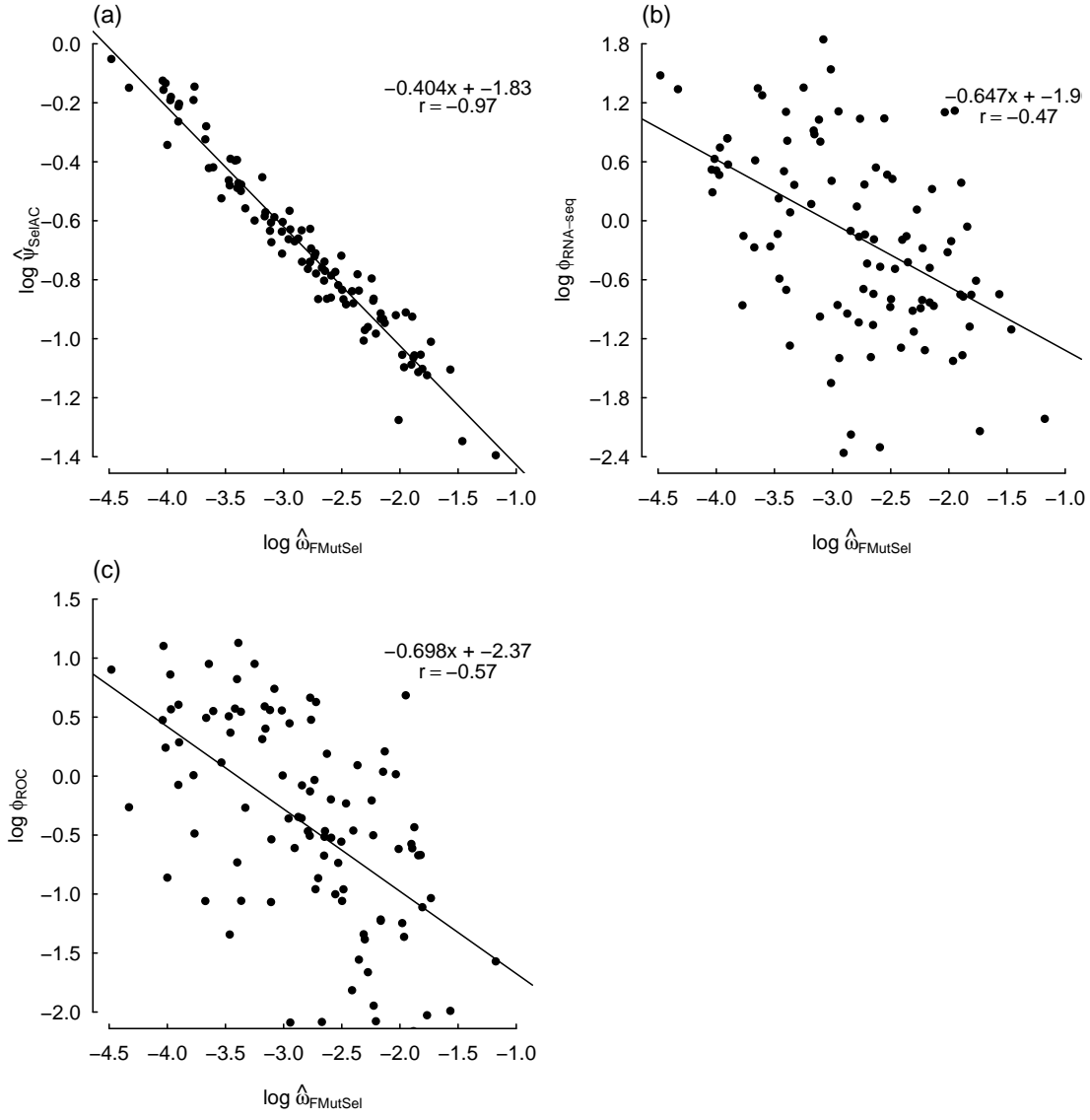


FIG. 3. Comparisons between ω_{FMutSel} , which is the nonsynonymous/synonymous mutation ratio in FMutSel, SelAC+ Γ estimates of protein functionality production rates $\hat{\psi}_{\text{SelAC}}$ (a), RNA-Seq based measurements of mRNA abundance $\phi_{\text{RNA-seq}}$ (b), and ROC-SEMPER's estimates of protein translation rates ϕ_{ROC} , which are based solely on *S. cerevisiae*'s patterns of codon usage bias (c), for *S. cerevisiae* across the 100 selected genes from ?. As in Figure ??, the equations in the upper right hand corner of each panel provide the regression fit and correlation coefficient.

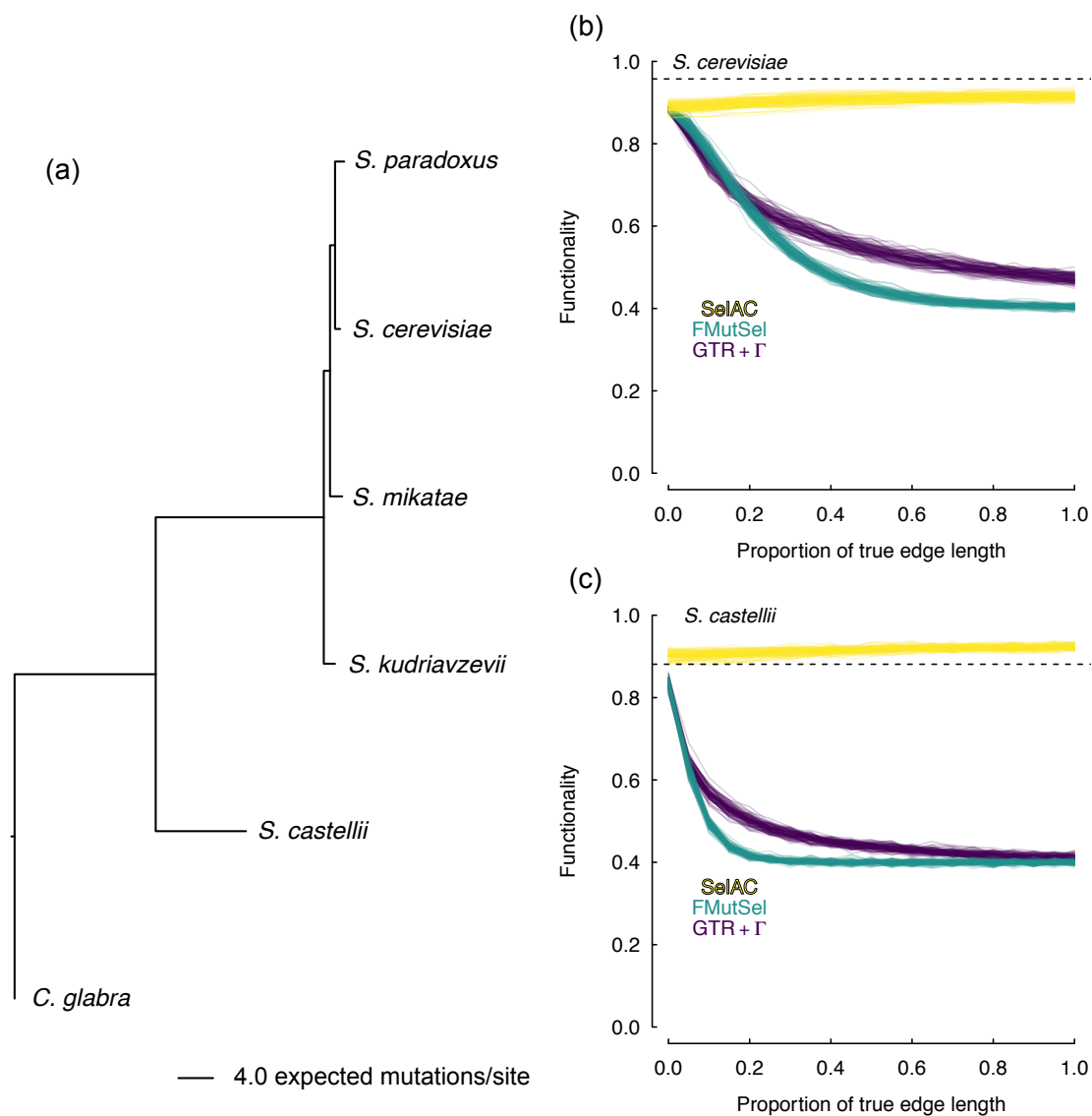


FIG. 4. (a) Maximum likelihood estimates of branch lengths under SelAC+ Γ for 100 selected genes from ?. Tests of model adequacy for *S. cerevisiae* (b) and *S. castellii* (c) indicated that, when these taxa are removed from the tree, and their sequences are simulated, the parameters of SelAC+ Γ exhibit functionality $\mathbf{B}(\vec{a}_{\text{obs}}|\vec{a}^*)$ that is far closer to the observed (dashed black line) than data sets produced from parameters of either FMutSel or GTR + Γ .

Supporting Materials

Supporting Materials for *Population Genetics Based Phylogenetics Under Stabilizing Selection for an Optimal Amino Acid Sequence: A Nested Modeling Approach* by Beaulieu *et al.* (In Review).

Comparisons of SelAC gene expression estimates with empirical measurements

In our model, the parameter ϕ measures the realized average protein synthesis rate of a gene. We compared our estimates of ϕ to two separate measures of gene expression, one empirical (Figure ??), and one model-based prediction that does not account for shared ancestry, for individual yeast taxa across the same set of genes. Our estimates of ϕ are positively correlated with both measures, which are also reasonably well correlated with each other (Figure ?? - ??) On the whole, these comparisons indicate not only a high degree of consistency among all three measures, but also, importantly, that estimates of ϕ obtained from SelAC provide real biological insight into the expression level of a gene.

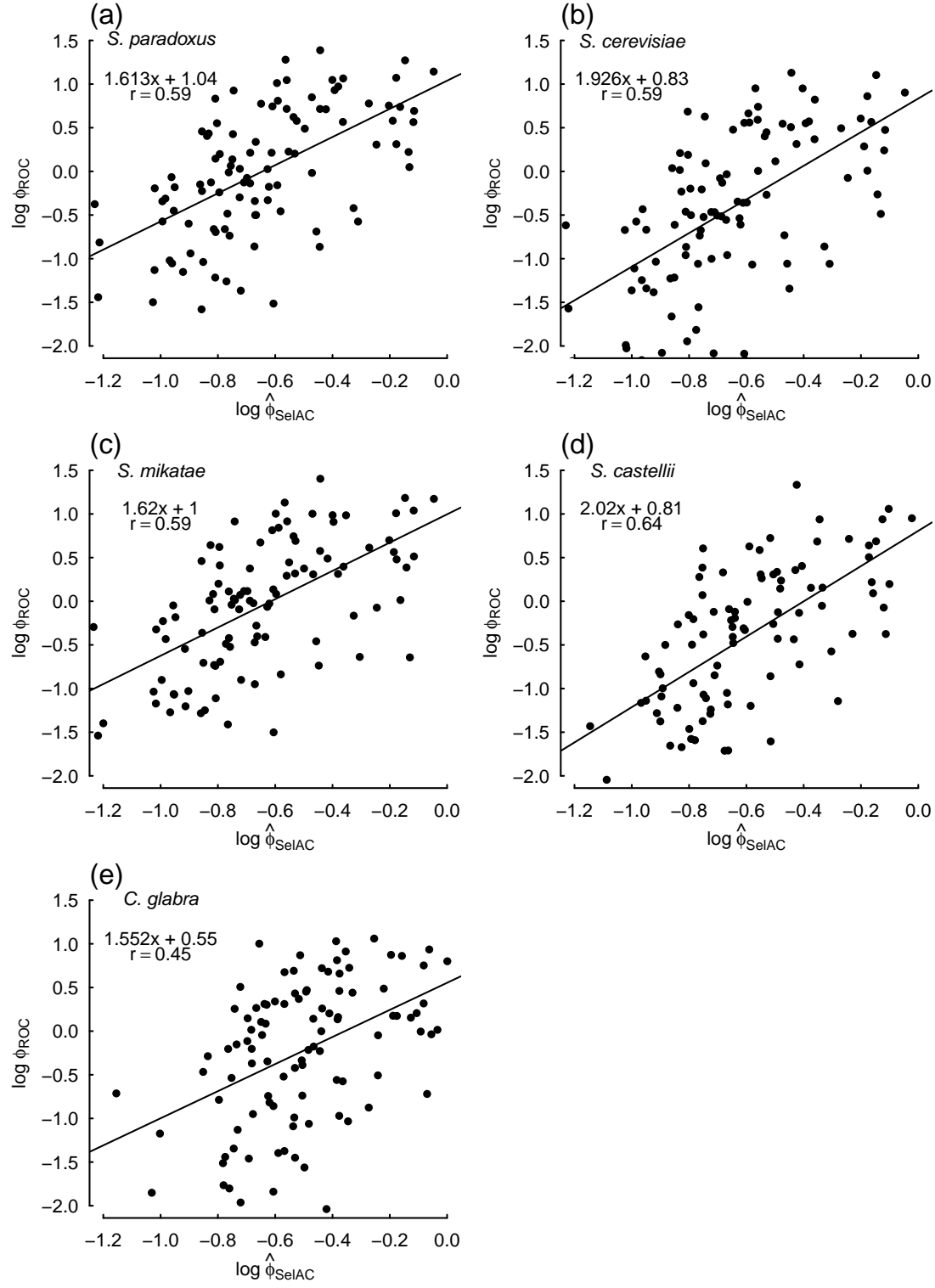


FIG. S1. Comparisons between estimates of ϕ obtained from SelAC+ Γ and the predicted gene expression from the ROC SEMPER model (?) for individual yeast taxa across the 100 selected genes from ?. As with figures in the main text, estimates

of ϕ were obtained by solving for ψ based on estimates of ψ' , and then dividing by $\mathbf{B}(\bar{a}_i|\bar{a}^*)$. The equations in the upper left hand corner of each panel represent the regression fit and correlation coefficient.

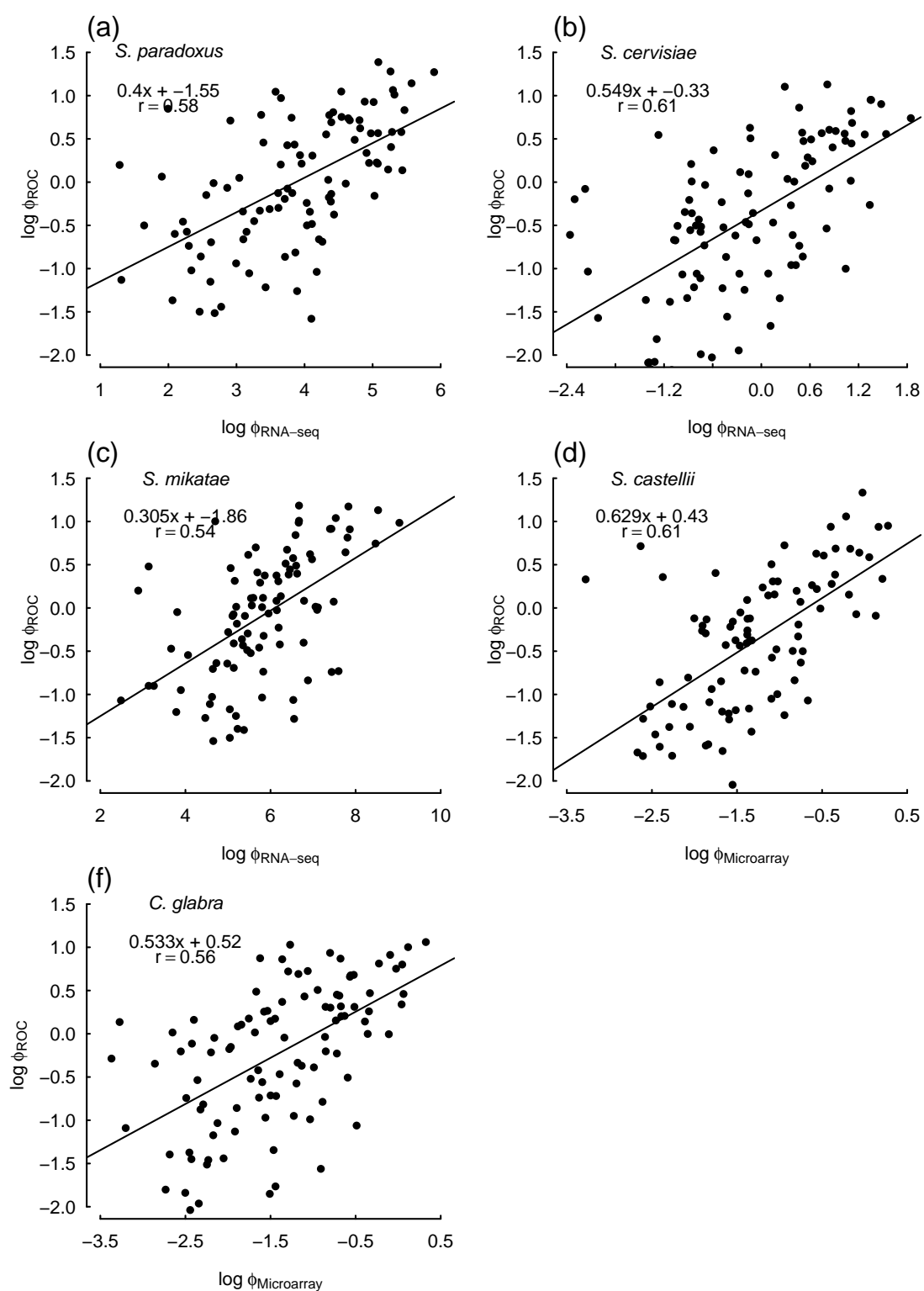


FIG. S2. Comparisons of predicted gene expression from the ROC SEMPER model (?) and direct measurements of expression from RNA-Seq or microarray data for individual yeast taxa across the 100 selected genes from ?. The equations in the upper left hand corner of each panel represent the regression fit and correlation coefficient.

TABLE

Table S1.: Comparison of SelAC to 163 other phylogenetic models to 100 selected genes from 6 yeast taxa ? using negative log likelihood ($-\ln(\mathcal{L})$), AIC, and AICc values. See Table ?? for more details Models of Rank 1-4, 88, and 166 were fitted using the SelAC software package. All remaining models were fitted using IQTree (?). Note that there are no models in common between IQTree and SelAC. SelAC's GY and IQTree's GY+F are the most similar. However, SelAC's GY uses a mutation model to generate expected codon frequencies while IQTree's GY+F uses the observed frequencies.

| | Rank | Model | $-\ln(\mathcal{L})$ | df | AIC | AICc | ΔAIC | ΔAICc |
|----|-------------------------------|-------|---------------------|--------|-----------|-----------|--------------------|---------------------|
| 1 | SelAC+ Γ | | 453,621 | 50,005 | 1,007,252 | 1,027,314 | 0 | 0 |
| 2 | SelAC | | 464,115 | 50,004 | 1,028,238 | 1,050,286 | 20,986 | 22,972 |
| 3 | SelAC _M + Γ | | 465,302 | 50,005 | 1,056,613 | 1,076,674 | 49,361 | 49,360 |
| 4 | FMutSel | | 597,141 | 178 | 1,194,637 | 1,194,638 | 187,385 | 167,324 |
| 5 | KOSI07+F+R10 | | 598,031 | 87 | 1,196,235 | 1,196,236 | 188,983 | 168,922 |
| 6 | KOSI07+F+R9 | | 598,326 | 85 | 1,196,822 | 1,196,822 | 189,570 | 169,508 |
| 7 | KOSI07+F+R8 | | 598,609 | 83 | 1,197,383 | 1,197,384 | 190,131 | 170,070 |
| 8 | KOSI07+F+R7 | | 598,940 | 81 | 1,198,041 | 1,198,041 | 190,789 | 170,727 |
| 9 | GY+F+R5 | | 599,010 | 79 | 1,198,178 | 1,198,179 | 190,926 | 170,865 |
| 10 | GY+F+R4 | | 599,017 | 77 | 1,198,188 | 1,198,188 | 190,936 | 170,874 |
| 11 | GY+F+R3 | | 599,092 | 75 | 1,198,334 | 1,198,334 | 191,082 | 171,020 |
| 12 | KOSI07+F+R6 | | 599,337 | 79 | 1,198,832 | 1,198,832 | 191,580 | 171,518 |
| 13 | GY+F+R2 | | 599,662 | 73 | 1,199,471 | 1,199,471 | 192,219 | 172,157 |
| 14 | KOSI07+F+R5 | | 599,854 | 77 | 1,199,862 | 1,199,862 | 192,610 | 172,548 |
| 15 | KOSI07+F+R4 | | 600,572 | 75 | 1,201,293 | 1,201,294 | 194,041 | 173,980 |
| 16 | GY+F+G4 | | 600,946 | 72 | 1,202,037 | 1,202,037 | 194,785 | 174,723 |
| 17 | GY+F+I+G4 | | 600,947 | 73 | 1,202,040 | 1,202,040 | 194,788 | 174,726 |

Continued on next page

Table S1 – *Continued from previous page*

| | Rank | Model | $-\ln(\mathcal{L})$ | df | AIC | AICc | ΔAIC | ΔAICc |
|----|------|-----------------|---------------------|----|-----------|-----------|--------------------|---------------------|
| 18 | | SCHN05+F+R10 | 601,260 | 87 | 1,202,694 | 1,202,694 | 195,442 | 175,380 |
| 19 | | KOSI07+F+R3 | 601,538 | 73 | 1,203,222 | 1,203,222 | 195,970 | 175,908 |
| 20 | | SCHN05+F+R9 | 602,116 | 85 | 1,204,402 | 1,204,402 | 197,150 | 177,088 |
| 21 | | KOSI07+F+R2 | 603,128 | 71 | 1,206,397 | 1,206,397 | 199,145 | 179,083 |
| 22 | | SCHN05+F+R8 | 603,280 | 83 | 1,206,725 | 1,206,726 | 199,473 | 179,412 |
| 23 | | KOSI07+F+G4 | 604,152 | 70 | 1,208,444 | 1,208,445 | 201,192 | 181,131 |
| 24 | | KOSI07+F+I+G4 | 604,152 | 71 | 1,208,446 | 1,208,446 | 201,194 | 181,132 |
| 25 | | SCHN05+F+R7 | 604,739 | 81 | 1,209,639 | 1,209,639 | 202,387 | 182,325 |
| 26 | | KOSI07+F3X4+R9 | 605,979 | 34 | 1,212,026 | 1,212,026 | 204,774 | 184,712 |
| 27 | | MGK+F3X4+R5 | 606,033 | 28 | 1,212,121 | 1,212,121 | 204,869 | 184,807 |
| 28 | | MGK+F3X4+R4 | 606,037 | 26 | 1,212,127 | 1,212,127 | 204,875 | 184,813 |
| 29 | | MGK+F3X4+R3 | 606,057 | 24 | 1,212,163 | 1,212,163 | 204,911 | 184,849 |
| 30 | | GY+F3X4+R5 | 606,154 | 28 | 1,212,364 | 1,212,364 | 205,112 | 185,050 |
| 31 | | GY+F3X4+R6 | 606,153 | 30 | 1,212,365 | 1,212,365 | 205,113 | 185,051 |
| 32 | | GY+F3X4+R4 | 606,181 | 26 | 1,212,414 | 1,212,414 | 205,162 | 185,100 |
| 33 | | GY+F3X4+R3 | 606,212 | 24 | 1,212,472 | 1,212,472 | 205,220 | 185,158 |
| 34 | | SCHN05+F+R6 | 606,181 | 79 | 1,212,520 | 1,212,520 | 205,268 | 185,206 |
| 35 | | KOSI07+F3X4+R8 | 606,322 | 32 | 1,212,708 | 1,212,708 | 205,456 | 185,394 |
| 36 | | KOSI07+F3X4+R7 | 606,913 | 30 | 1,213,886 | 1,213,886 | 206,634 | 186,572 |
| 37 | | MGK+F3X4+R2 | 606,960 | 22 | 1,213,965 | 1,213,965 | 206,713 | 186,651 |
| 38 | | SCHN05+F3X4+R10 | 607,042 | 36 | 1,214,155 | 1,214,155 | 206,903 | 186,841 |
| 39 | | GY+F3X4+R2 | 607,143 | 22 | 1,214,329 | 1,214,329 | 207,077 | 187,015 |
| 40 | | SCHN05+F+R5 | 607,190 | 77 | 1,214,533 | 1,214,534 | 207,281 | 187,220 |
| 41 | | SCHN05+F3X4+R9 | 607,253 | 34 | 1,214,573 | 1,214,573 | 207,321 | 187,259 |
| 42 | | KOSI07+F3X4+R6 | 607,321 | 28 | 1,214,697 | 1,214,697 | 207,445 | 187,383 |
| 43 | | KOSI07+F3X4+R10 | 607,370 | 36 | 1,214,812 | 1,214,812 | 207,560 | 187,498 |
| 44 | | SCHN05+F3X4+R8 | 607,638 | 32 | 1,215,339 | 1,215,339 | 208,087 | 188,025 |
| 45 | | MGK+F3X4+G4 | 607,662 | 21 | 1,215,365 | 1,215,365 | 208,113 | 188,051 |

Continued on next page

Table S1 – *Continued from previous page*

| | Rank | Model | $-\ln(\mathcal{L})$ | df | AIC | AICc | ΔAIC | ΔAICc | |
|----|------|----------------|---------------------|----|-----------|-----------|--------------------|---------------------|--|
| 46 | | MGK+F3X4+I+G4 | 607,663 | 22 | 1,215,370 | 1,215,370 | 208,118 | 188,056 | |
| 47 | | GY+F+I | 607,640 | 72 | 1,215,424 | 1,215,424 | 208,172 | 188,110 | |
| 48 | | GY+F3X4+G4 | 607,743 | 21 | 1,215,527 | 1,215,527 | 208,275 | 188,213 | |
| 49 | | GY+F3X4+I+G4 | 607,744 | 22 | 1,215,531 | 1,215,531 | 208,279 | 188,217 | |
| 50 | | KOSI07+F3X4+R5 | 607,829 | 26 | 1,215,709 | 1,215,709 | 208,457 | 188,395 | |
| 51 | | SCHN05+F+R4 | 607,792 | 75 | 1,215,734 | 1,215,735 | 208,482 | 188,421 | |
| 52 | | SCHN05+F3X4+R7 | 608,418 | 30 | 1,216,897 | 1,216,897 | 209,645 | 189,583 | |
| 53 | | SCHN05+F+R3 | 608,416 | 73 | 1,216,977 | 1,216,977 | 209,725 | 189,663 | |
| 54 | | KOSI07+F3X4+R4 | 608,554 | 24 | 1,217,156 | 1,217,156 | 209,904 | 189,842 | |
| 55 | | GY+F | 608,565 | 71 | 1,217,273 | 1,217,273 | 210,021 | 189,959 | |
| 56 | | GY+F1X4+R6 | 608,839 | 24 | 1,217,726 | 1,217,726 | 210,474 | 190,412 | |
| 57 | | GY+F1X4+R5 | 608,842 | 22 | 1,217,728 | 1,217,728 | 210,476 | 190,414 | |
| 58 | | GY+F1X4+R4 | 608,866 | 20 | 1,217,772 | 1,217,772 | 210,520 | 190,458 | |
| 59 | | MGK+F1X4+R5 | 608,879 | 22 | 1,217,802 | 1,217,802 | 210,550 | 190,488 | |
| 60 | | MGK+F1X4+R4 | 608,883 | 20 | 1,217,807 | 1,217,807 | 210,555 | 190,493 | |
| 61 | | GY+F1X4+R3 | 608,889 | 18 | 1,217,813 | 1,217,813 | 210,561 | 190,499 | |
| 62 | | MGK+F1X4+R3 | 608,907 | 18 | 1,217,851 | 1,217,851 | 210,599 | 190,537 | |
| 63 | | SCHN05+F+R2 | 609,165 | 71 | 1,218,472 | 1,218,472 | 211,220 | 191,158 | |
| 64 | | KOSI07+F3X4+R3 | 609,569 | 22 | 1,219,182 | 1,219,182 | 211,930 | 191,868 | |
| 65 | | SCHN05+F3X4+R6 | 609,687 | 28 | 1,219,430 | 1,219,430 | 212,178 | 192,116 | |
| 66 | | GY+F1X4+R2 | 609,813 | 16 | 1,219,659 | 1,219,659 | 212,407 | 192,345 | |
| 67 | | MGK+F1X4+R2 | 609,820 | 16 | 1,219,672 | 1,219,672 | 212,420 | 192,358 | |
| 68 | | SCHN05+F+G4 | 610,131 | 70 | 1,220,401 | 1,220,401 | 213,149 | 193,087 | |
| 69 | | SCHN05+F+I+G4 | 610,131 | 71 | 1,220,403 | 1,220,403 | 213,151 | 193,089 | |
| 70 | | GY+F1X4+G4 | 610,207 | 15 | 1,220,444 | 1,220,444 | 213,192 | 193,130 | |
| 71 | | GY+F1X4+I+G4 | 610,208 | 16 | 1,220,447 | 1,220,447 | 213,195 | 193,133 | |
| 72 | | MGK+F1X4+G4 | 610,273 | 15 | 1,220,575 | 1,220,575 | 213,323 | 193,261 | |
| 73 | | MGK+F1X4+I+G4 | 610,274 | 16 | 1,220,580 | 1,220,580 | 213,328 | 193,266 | |

Continued on next page

Table S1 – *Continued from previous page*

| | Rank | Model | $-\ln(\mathcal{L})$ | df | AIC | AICc | ΔAIC | ΔAICc |
|-----|------|------------------|---------------------|-----|-----------|-----------|--------------------|---------------------|
| 74 | | KOSI07+F+I | 610,257 | 70 | 1,220,653 | 1,220,653 | 213,401 | 193,339 |
| 75 | | KOSI07+F1X4+R8 | 610,602 | 26 | 1,221,255 | 1,221,255 | 214,003 | 193,941 |
| 76 | | KOSI07+F | 611,155 | 69 | 1,222,448 | 1,222,448 | 215,196 | 195,134 |
| 77 | | KOSI07+F1X4+R7 | 611,353 | 24 | 1,222,755 | 1,222,755 | 215,503 | 195,441 |
| 78 | | SCHN05+F3X4+R5 | 611,498 | 26 | 1,223,048 | 1,223,048 | 215,796 | 195,734 |
| 79 | | KOSI07+F1X4+R6 | 611,809 | 22 | 1,223,662 | 1,223,662 | 216,410 | 196,348 |
| 80 | | KOSI07+F3X4+R2 | 611,865 | 20 | 1,223,769 | 1,223,769 | 216,517 | 196,455 |
| 81 | | MG+F3X4+R7 | 612,290 | 31 | 1,224,642 | 1,224,642 | 217,390 | 197,328 |
| 82 | | MG+F3X4+R8 | 612,289 | 33 | 1,224,645 | 1,224,645 | 217,393 | 197,331 |
| 83 | | KOSI07+F1X4+R5 | 612,311 | 20 | 1,224,662 | 1,224,662 | 217,410 | 197,348 |
| 84 | | MG+F3X4+R6 | 612,313 | 29 | 1,224,683 | 1,224,683 | 217,431 | 197,369 |
| 85 | | MG+F3X4+R5 | 612,336 | 27 | 1,224,725 | 1,224,725 | 217,473 | 197,411 |
| 86 | | MG+F3X4+R4 | 612,355 | 25 | 1,224,760 | 1,224,760 | 217,508 | 197,446 |
| 87 | | MG+F3X4+R3 | 612,369 | 23 | 1,224,783 | 1,224,783 | 217,531 | 197,469 |
| 88 | | GY | 612,670 | 111 | 1,225,563 | 1,225,563 | 218,311 | 198,249 |
| 89 | | KOSI07+F3X4+G4 | 612,932 | 19 | 1,225,903 | 1,225,903 | 218,651 | 198,589 |
| 90 | | KOSI07+F3X4+I+G4 | 612,932 | 20 | 1,225,905 | 1,225,905 | 218,653 | 198,591 |
| 91 | | SCHN05+F1X4+R10 | 612,982 | 30 | 1,226,024 | 1,226,024 | 218,772 | 198,710 |
| 92 | | KOSI07+F1X4+R4 | 612,995 | 18 | 1,226,025 | 1,226,026 | 218,773 | 198,712 |
| 93 | | MG+F3X4+R2 | 613,159 | 21 | 1,226,360 | 1,226,360 | 219,108 | 199,046 |
| 94 | | MGK+F3X4+I | 613,206 | 21 | 1,226,454 | 1,226,454 | 219,202 | 199,140 |
| 95 | | KOSI07+F1X4+R9 | 613,259 | 28 | 1,226,574 | 1,226,574 | 219,322 | 199,260 |
| 96 | | SCHN05+F1X4+R9 | 613,320 | 28 | 1,226,696 | 1,226,696 | 219,444 | 199,382 |
| 97 | | SCHN05+F3X4+R4 | 613,713 | 24 | 1,227,474 | 1,227,474 | 220,222 | 200,160 |
| 98 | | SCHN05+F1X4+R8 | 613,817 | 26 | 1,227,686 | 1,227,686 | 220,434 | 200,372 |
| 99 | | MG+F3X4+G4 | 613,854 | 20 | 1,227,747 | 1,227,747 | 220,495 | 200,433 |
| 100 | | MG+F3X4+I+G4 | 613,856 | 21 | 1,227,753 | 1,227,753 | 220,501 | 200,439 |
| 101 | | KOSI07+FU+R6 | 614,272 | 19 | 1,228,581 | 1,228,581 | 221,329 | 201,267 |

Continued on next page

Table S1 – *Continued from previous page*

| | Rank | Model | $-\ln(\mathcal{L})$ | df | AIC | AICc | ΔAIC | ΔAICc | |
|-----|------|----------------|---------------------|----|-----------|-----------|--------------------|---------------------|--|
| 102 | | KOSI07+FU+R5 | 614,454 | 17 | 1,228,942 | 1,228,942 | 221,690 | 201,628 | |
| 103 | | GY+F3X4+I | 614,457 | 21 | 1,228,957 | 1,228,957 | 221,705 | 201,643 | |
| 104 | | SCHN05+F1X4+R7 | 614,535 | 24 | 1,229,119 | 1,229,119 | 221,867 | 201,805 | |
| 105 | | KOSI07+F1X4+R3 | 614,556 | 16 | 1,229,144 | 1,229,144 | 221,892 | 201,830 | |
| 106 | | MGK+F3X4 | 614,642 | 20 | 1,229,325 | 1,229,325 | 222,073 | 202,011 | |
| 107 | | KOSI07+FU+R7 | 614,772 | 21 | 1,229,586 | 1,229,586 | 222,334 | 202,272 | |
| 108 | | SCHN05+F1X4+R6 | 615,584 | 22 | 1,231,212 | 1,231,212 | 223,960 | 203,898 | |
| 109 | | MG+F1X4+R4 | 615,590 | 19 | 1,231,217 | 1,231,217 | 223,965 | 203,903 | |
| 110 | | MG+F1X4+R3 | 615,596 | 17 | 1,231,225 | 1,231,225 | 223,973 | 203,911 | |
| 111 | | MGK+F1X4+I | 615,826 | 15 | 1,231,682 | 1,231,682 | 224,430 | 204,368 | |
| 112 | | GY+F3X4 | 615,827 | 20 | 1,231,694 | 1,231,694 | 224,442 | 204,380 | |
| 113 | | KOSI07+FU+R4 | 615,916 | 15 | 1,231,862 | 1,231,862 | 224,610 | 204,548 | |
| 114 | | SCHN05+F3X4+R3 | 616,067 | 22 | 1,232,178 | 1,232,178 | 224,926 | 204,864 | |
| 115 | | GY+F1X4+I | 616,171 | 15 | 1,232,372 | 1,232,372 | 225,120 | 205,058 | |
| 116 | | MG+F1X4+R2 | 616,483 | 15 | 1,232,997 | 1,232,997 | 225,745 | 205,683 | |
| 117 | | MG+F1X4+G4 | 616,887 | 14 | 1,233,801 | 1,233,801 | 226,549 | 206,487 | |
| 118 | | MG+F1X4+I+G4 | 616,889 | 15 | 1,233,808 | 1,233,808 | 226,556 | 206,494 | |
| 119 | | SCHN05+F1X4+R5 | 617,068 | 20 | 1,234,176 | 1,234,176 | 226,924 | 206,862 | |
| 120 | | KOSI07+FU+R3 | 617,300 | 13 | 1,234,626 | 1,234,626 | 227,374 | 207,312 | |
| 121 | | MGK+F1X4 | 617,351 | 14 | 1,234,730 | 1,234,730 | 227,478 | 207,416 | |
| 122 | | GY+F1X4 | 617,744 | 14 | 1,235,515 | 1,235,515 | 228,263 | 208,201 | |
| 123 | | KOSI07+F3X4+I | 618,072 | 19 | 1,236,181 | 1,236,182 | 228,929 | 208,868 | |
| 124 | | SCHN05+F1X4+R4 | 618,974 | 18 | 1,237,984 | 1,237,984 | 230,732 | 210,670 | |
| 125 | | MG+F3X4+I | 619,182 | 20 | 1,238,403 | 1,238,403 | 231,151 | 211,089 | |
| 126 | | KOSI07+F3X4 | 619,604 | 18 | 1,239,244 | 1,239,244 | 231,992 | 211,930 | |
| 127 | | KOSI07+F1X4+R2 | 619,779 | 14 | 1,239,585 | 1,239,585 | 232,333 | 212,271 | |
| 128 | | SCHN05+F+I | 619,826 | 70 | 1,239,792 | 1,239,792 | 232,540 | 212,478 | |
| 129 | | MG+F3X4 | 620,567 | 19 | 1,241,172 | 1,241,172 | 233,920 | 213,858 | |

Continued on next page

Table S1 – *Continued from previous page*

| | Rank | Model | $-\ln(\mathcal{L})$ | df | AIC | AICc | ΔAIC | ΔAICc |
|-----|------|------------------|---------------------|----|-----------|-----------|--------------------|---------------------|
| 130 | | SCHN05+F | 620,670 | 69 | 1,241,477 | 1,241,477 | 234,225 | 214,163 |
| 131 | | KOSI07+F1X4+G4 | 620,863 | 13 | 1,241,751 | 1,241,751 | 234,499 | 214,437 |
| 132 | | KOSI07+F1X4+I+G4 | 620,862 | 14 | 1,241,753 | 1,241,753 | 234,501 | 214,439 |
| 133 | | SCHN05+F1X4+R3 | 621,059 | 16 | 1,242,150 | 1,242,150 | 234,898 | 214,836 |
| 134 | | MG+F1X4+I | 622,158 | 14 | 1,244,344 | 1,244,344 | 237,092 | 217,030 |
| 135 | | KOSI07+FU+R2 | 622,429 | 11 | 1,244,879 | 1,244,879 | 237,627 | 217,565 |
| 136 | | SCHN05+F3X4+R2 | 623,050 | 20 | 1,246,140 | 1,246,140 | 238,888 | 218,826 |
| 137 | | SCHN05+FU+R10 | 623,378 | 27 | 1,246,810 | 1,246,810 | 239,558 | 219,496 |
| 138 | | SCHN05+F1X4+R2 | 623,541 | 14 | 1,247,111 | 1,247,111 | 239,859 | 219,797 |
| 139 | | MG+F1X4 | 623,675 | 13 | 1,247,376 | 1,247,376 | 240,124 | 220,062 |
| 140 | | SCHN05+FU+R9 | 623,893 | 25 | 1,247,836 | 1,247,836 | 240,584 | 220,522 |
| 141 | | KOSI07+FU+G4 | 624,314 | 10 | 1,248,647 | 1,248,647 | 241,395 | 221,333 |
| 142 | | KOSI07+FU+I+G4 | 624,313 | 11 | 1,248,647 | 1,248,647 | 241,395 | 221,333 |
| 143 | | SCHN05+F1X4+G4 | 624,399 | 13 | 1,248,823 | 1,248,823 | 241,571 | 221,509 |
| 144 | | SCHN05+F1X4+I+G4 | 624,398 | 14 | 1,248,825 | 1,248,825 | 241,573 | 221,511 |
| 145 | | SCHN05+FU+R8 | 624,408 | 23 | 1,248,861 | 1,248,861 | 241,609 | 221,547 |
| 146 | | SCHN05+FU+R7 | 624,916 | 21 | 1,249,874 | 1,249,874 | 242,622 | 222,560 |
| 147 | | KOSI07+F1X4+I | 625,424 | 13 | 1,250,875 | 1,250,875 | 243,623 | 223,561 |
| 148 | | SCHN05+FU+R6 | 625,486 | 19 | 1,251,009 | 1,251,009 | 243,757 | 223,695 |
| 149 | | SCHN05+FU+R5 | 626,269 | 17 | 1,252,572 | 1,252,572 | 245,320 | 225,258 |
| 150 | | SCHN05+F3X4+G4 | 626,387 | 19 | 1,252,812 | 1,252,812 | 245,560 | 225,498 |
| 151 | | SCHN05+F3X4+I+G4 | 626,387 | 20 | 1,252,813 | 1,252,813 | 245,561 | 225,499 |
| 152 | | KOSI07+F1X4 | 627,290 | 12 | 1,254,605 | 1,254,605 | 247,353 | 227,291 |
| 153 | | SCHN05+FU+R4 | 627,433 | 15 | 1,254,896 | 1,254,896 | 247,644 | 227,582 |
| 154 | | KOSI07+FU+I | 627,802 | 10 | 1,255,624 | 1,255,624 | 248,372 | 228,310 |
| 155 | | SCHN05+FU+R3 | 628,994 | 13 | 1,258,014 | 1,258,014 | 250,762 | 230,700 |
| 156 | | KOSI07+FU | 630,149 | 9 | 1,260,316 | 1,260,316 | 253,064 | 233,002 |
| 157 | | SCHN05+FU+R2 | 632,325 | 11 | 1,264,673 | 1,264,673 | 257,421 | 237,359 |

Continued on next page

Table S1 – *Continued from previous page*

| | Rank | Model | $-\ln(\mathcal{L})$ | df | AIC | AICc | ΔAIC | ΔAICc | |
|-----|------|----------------|---------------------|-----|-----------|-----------|--------------------|---------------------|--|
| 158 | | SCHN05+F3X4+I | 632,477 | 19 | 1,264,991 | 1,264,991 | 257,739 | 237,677 | |
| 159 | | SCHN05+F1X4+I | 633,183 | 13 | 1,266,392 | 1,266,392 | 259,140 | 239,078 | |
| 160 | | SCHN05+FU+G4 | 633,625 | 10 | 1,267,270 | 1,267,270 | 260,018 | 239,956 | |
| 161 | | SCHN05+FU+I+G4 | 633,625 | 11 | 1,267,272 | 1,267,272 | 260,020 | 239,958 | |
| 162 | | SCHN05+F3X4 | 633,952 | 18 | 1,267,940 | 1,267,940 | 260,688 | 240,626 | |
| 163 | | SCHN05+F1X4 | 635,039 | 12 | 1,270,102 | 1,270,102 | 262,850 | 242,788 | |
| 164 | | SCHN05+FU+I | 640,485 | 10 | 1,280,991 | 1,280,991 | 273,739 | 253,677 | |
| 165 | | SCHN05+FU | 643,334 | 9 | 1,286,686 | 1,286,686 | 279,434 | 259,372 | |
| 166 | | GTR+G | 655,116 | 610 | 1,311,553 | 1,311,554 | 304,301 | 284,240 | |

907 Simulations

908 As stated in the main text, overall, the simulation results indicate that the SelAC model can reasonably
 909 recover the known values of the generating model (Figure ?? - ??). This includes not only the parameters
 910 in SelAC, but also the optimal amino acids for a given sequence as well as the estimates of the branch
 911 lengths. Aside from the observations noted in the main text, a reviewer pointed out to us that it may
 912 also be difficult for SelAC to account for changing amino-acid, which we agree may also play a role. It
 913 has been suggested, in studies of the behavior of the gamma distribution in applications of nucleotide
 914 substitution model, that increasing the number of rate categories can often improve accuracy of the shape
 915 parameter (?). Future work will address this issue.

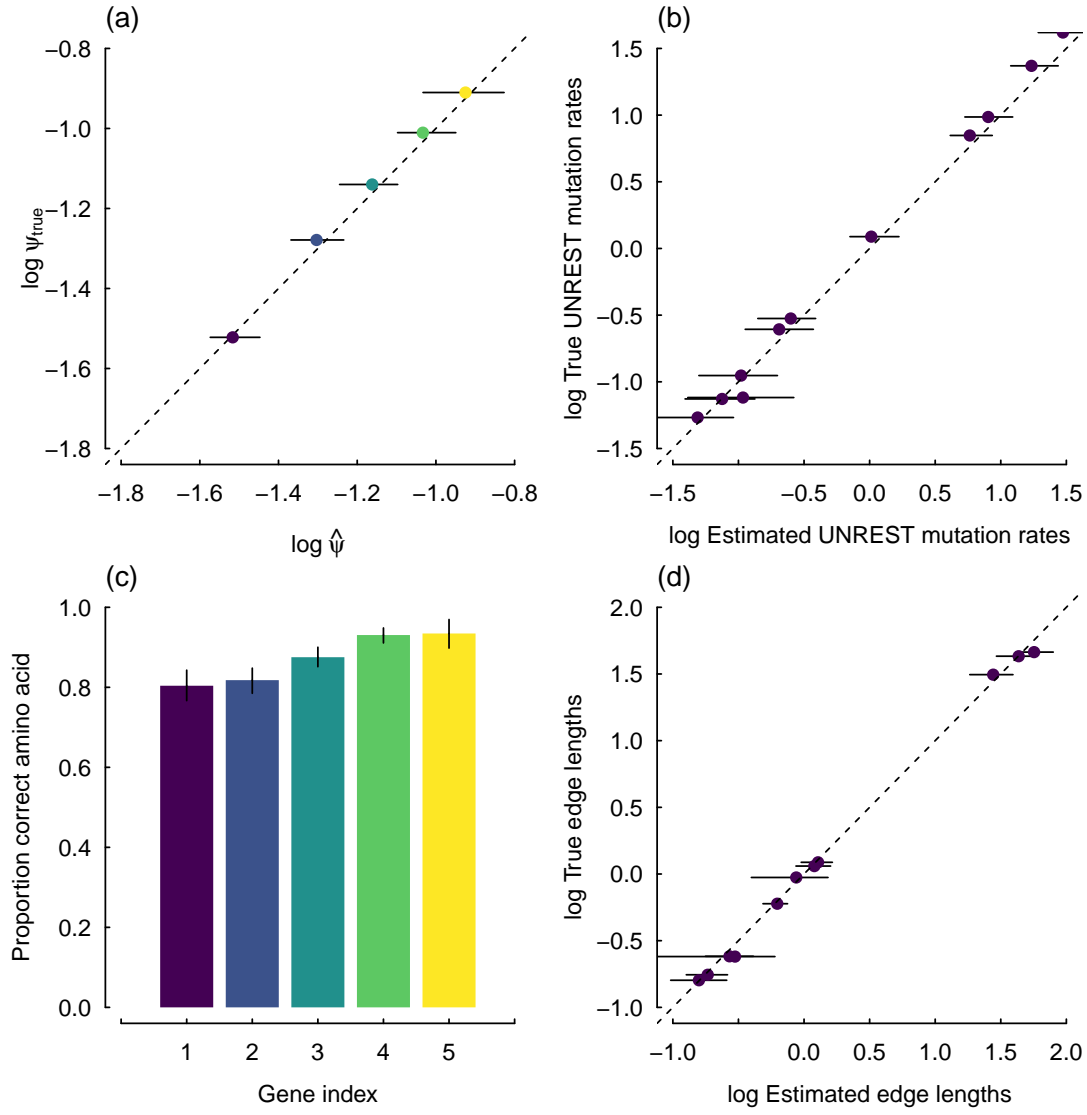


FIG. S3. Same figure as in Figure 1 in the main text, except the generating model does not include a site-specific sensitivity in the generating model (i.e., $\alpha_G = \infty$).

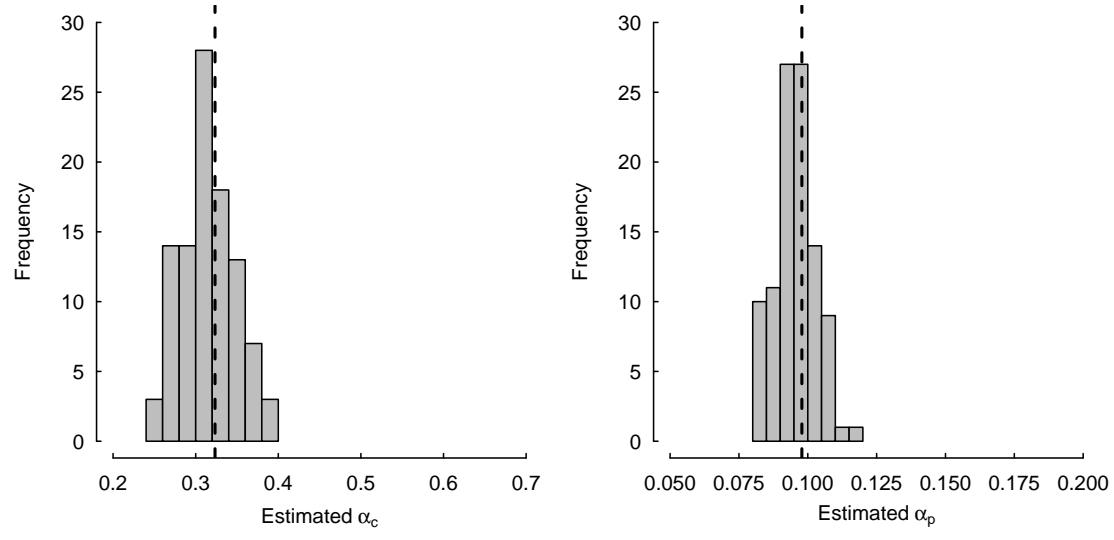


FIG. S4. The distribution of estimates of the Grantham weights, α_c and α_p , in a SelAC model, where we assume $\alpha_G = \infty$, and thus no site-specific sensitivity in the generating model. The dashed line represents the value used in the generating model.

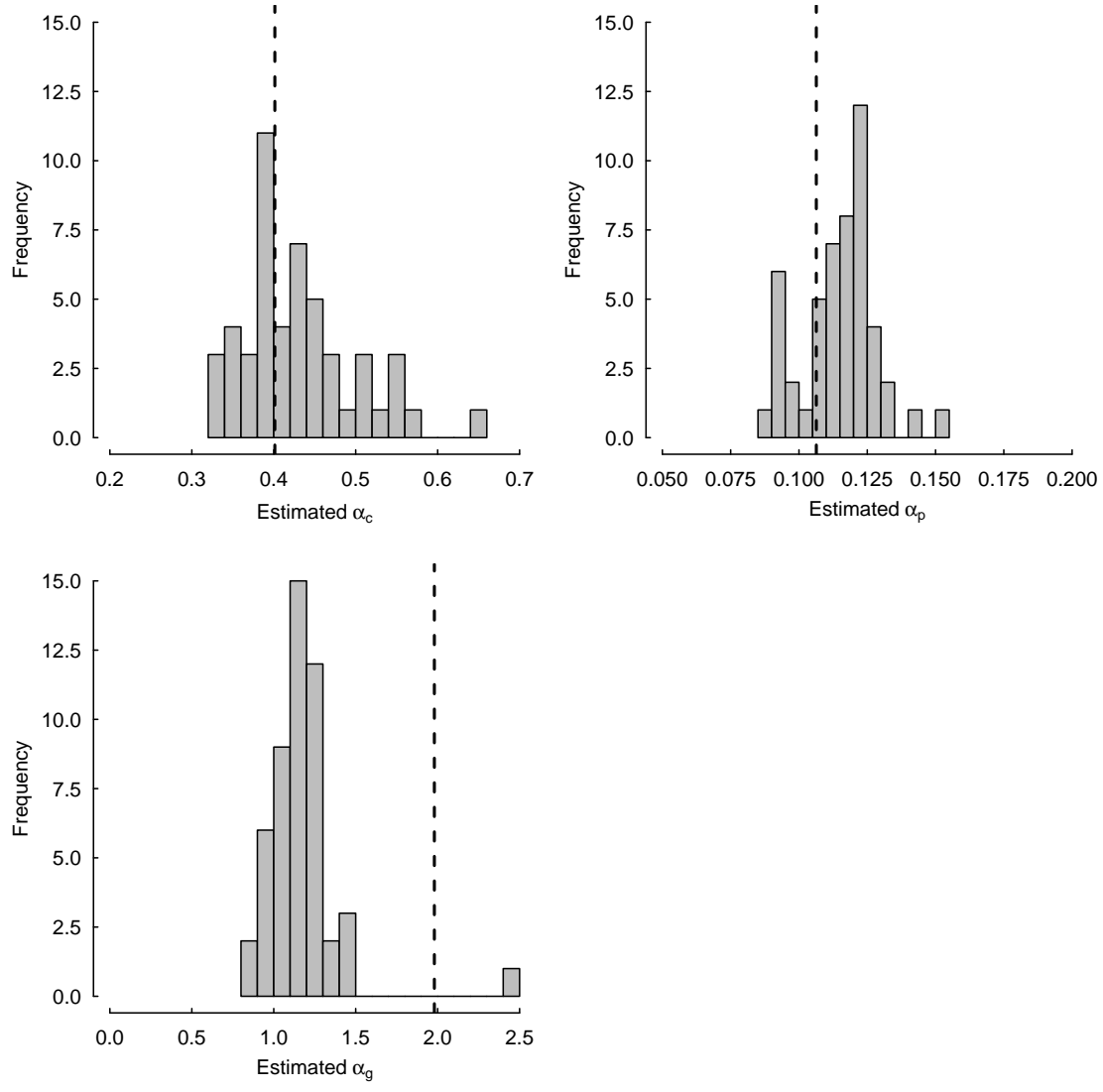


FIG. S5. Same figure as in Figure S4, except the generating model includes site-specific sensitivity in the generating model (i.e., α_G). Unlike, Grantham weights, which showed no systematic bias, there is a downward bias in estimates of α_G .